

1467-15851

DOUGLAS REPORT SM-49105-F2

CR 99054

CASE FILE
COPY

STRESS CORROSION CRACKING OF TITANIUM
ALLOYS AT AMBIENT TEMPERATURE
IN AQUEOUS SOLUTIONS

YEARLY SUMMARY REPORT
JULY 1967 THROUGH JUNE 1968
UNDER CONTRACT NAS 7-488

JULY 1968



Report SM-49105-F2

STRESS CORROSION CRACKING OF TITANIUM ALLOYS AT
AMBIENT TEMPERATURE IN AQUEOUS SOLUTIONS

Yearly Summary Report
July 1967 Through June 1968

Contract NAS 7-488

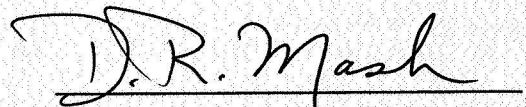
Administered by
Chief, Research SRT NASA Headquarters
Code RRM

Prepared by:



T. L. Mackay, Ph. D.
Senior Research Scientist

Approved by:



D. R. Mash, Ph. D.
Manager
Materials Research Department

MISSILE & SPACE SYSTEMS DIVISION
ASTROPOWER LABORATORY
McDonnell Douglas Corporation
Newport Beach, California

FOREWORD

This report was prepared by Astropower Laboratory, McDonnell Douglas Corporation, under NASA contract NAS 7-488. It is a yearly summary report and covers work conducted from July 1967 through June 1968. The work is administered by the Chief, Research SRT, NASA Headquarters, Code RRM, with Mr. Richard H. Raring as Project Scientist.

This report was prepared by Dr. T. L. Mackay and Dr. N. A. Tiner. Messrs. W. A. Cannon and R. G. Ingersoll have greatly contributed to the performance of this work.

ABSTRACT

Stress corrosion tests in aqueous salt solutions employing single edge notch specimens of Ti-8Al-1Mo-1V in duplex annealed, 1600°F and 1700°F solution annealed were susceptible to stress corrosion cracking (SCC) in aqueous salt solutions at ambient temperature. Martensitic structures obtained by annealing specimens at 1800°F or higher and containing hydrogen up to 100 ppm were immune to SCC in aqueous salt solution. The susceptibility of alpha-beta structures, obtained by reheating martensitic structures from 1800°F in the temperature range 900°F to 1450°F, to SCC was dependent on the strain rate. Specimens of Ti-8Al-1Mo-1V in duplex annealed or 1600°F solution heat treated condition, stress corrosion cracked in distilled water with 2% tritiated water, did not exhibit evidence of hydrogen pickup on the fractured faces by electron microautoradiography. An alpha alloy Ti-4Al, containing up to 150 ppm was immune to SCC, while Ti-8Al whether air quenched or water quenched from 1450°F was susceptible to SCC. Increasing aluminum content from 4 w/o to 8 w/o changes the dislocation arrangement from dislocation tangles to coplanar arrays in deformed material. In acicular martensitic structures, planar dislocation arrays are also observed; however, dislocation movement is restricted by retained beta with slip occurring simultaneously across several grains. The effect of aluminum appears to be related to the lowering of the stacking fault energy in alpha titanium and not to the ordering reaction.

CONTENTS

1.0	INTRODUCTION	1
2.0	EXPERIMENTAL EVALUATIONS	3
2.1	Effect of Microstructure and Hydrogen Content on Susceptibility to Stress Corrosion Cracking (SCC)	3
2.2	Microautoradiography Studies	11
2.3	Effect of Aluminum Content on Stress Corrosion Cracking	33
2.4	Transmission Electron Microscopy Studies	33
3.0	CONCLUSIONS	56
	REFERENCES	58

FIGURES

1	Microstructure of Ti-8Al-1Mo-1V Following Different Solution Heat Treatments	4
2	Electron Micrograph Illustrating the Fine Details of the Acicular Structure Shown in Figure 1d	8
3	Electron Micrographs Illustrating the Islands of Acicular Structure of Retained Beta (A) and Martensitic Alpha (B) in Equiaxial Alpha Matrix (C) as in Figure 1c	9
4	Effect of Stress Intensity on Time-to-Fracture for Ti-8Al-1Mo-1V, 1600°F Heat Treatment with 110 ppm Added H ₂ in 3% NaCl Solution	12
5	Electron Micrograph of Alloy Sample Solution-Annealed at 1800°F and Aged at 1450°F	13
6	Microautoradiograph of Tritium in Ti-8Al-1Mo-1V, 2000°F, 2 Hours, A. Q. + 1600°F, 2 Hours, A. Q. Containing 13 ppm	16
7	Microautoradiograph of Tritium in Ti-8Al-1Mo-1V, 2000°F, 2 Hours, A. Q. + 1600°F, 2 Hours, A. Q. Containing 40 ppm	17
8	Microautoradiograph of Tritium in Ti-3.1Al	18
9	Electron Microautoradiograph of Ti-8Al-1Mo-1V Alloy Containing 40 ppm Tritium in 1800°F Solution Annealed Condition	21
10	Electron Microautoradiograph of Tritium in Ti-8Al-1Mo-1V Alloy Solution Annealed at 1800°F and Stabilized at 1450°F, Then Tritium Charged at 1450°F	23
11	Electron Microautoradiograph of Tritium in Ti-8Al-1Mo-1V Alloy Solution Annealed at 1800°F and Aged at 900°F, Then Tritium Charged at 900°F	24
12	Electron Microautoradiograph Illustrating Tritium Segregation in Fractured Beta Grain Surface of Ti-6Al-4V Alloy, 30 ppm Tritium Gas Charged and Fractured in Air	26
13	Electron Microautoradiograph of Ti-8Al-1Mo-1V Alloy, Duplex Annealed, Fracture Face Stress Corrosion Cracked in 2% Tritiated Water	27
14	Electron Microautoradiograph of Ti-8Al-1Mo-1V Alloy, Duplex Annealed, Fracture Face Stress Corrosion Cracked in 3% Aqueous Salt Solution with 2% Tritiated Water	28
15	Electron Microautoradiograph of Ti-8Al-1Mo-1V Alloy, 1600°F Solution Annealed, Fracture Face Stress Corrosion Cracked in 3% Aqueous Salt Solution with 2% Tritiated Water	29
16	Electron Microautoradiograph of 5 Al-2.5 Charged with 40 ppm Tritium at 1450°F, Fracture Face Stress Corrosion Cracked in 3% Aqueous Salt Solution	30

17	Electron Microautoradiograph of Ti-8Al, Charged with 30 ppm of Tritium at 1450°F, Fracture Face Stress Corrosion Cracked in 3% Aqueous Salt Solution	31
18	Electron Microautoradiograph of Ti-8Al-1Mo-1V, Charged with 30 ppm Tritium at 1450°F, Fracture Face Stress Corrosion Cracked in 3% Aqueous Salt Solution	32
19	Microstructure of Titanium-Aluminum Alloys	34
20	Transmission Electron Micrograph of Ti-8Al-1Mo-1V, Duplex Annealed	38
21	Transmission Electron Micrograph of Ti-6Al-4V	39
22	Transmission Electron Micrograph of Ti-5Al-2.5Sn	40
23	Transmission Electron Micrograph of Ti-5Al-2.5Sn Following Stress and 2-Minute Immersion in 5% NaCl Solution	41
24	Transmission Electron Micrograph of Ti-8Al-1Mo-1V Following Stress and 8-Minute Immersion in 5% NaCl Solution	42
25	Transmission Electron Micrograph of Stressed Ti-6Al-4V Following Stress and 45-Minute Immersion in 5% NaCl Solution	43
26	Transmission Electron Micrograph of Annealed Ti-4Al Alloy	45
27	Transmission Electron Micrograph of Annealed Ti-8Al Alloy	46
28	Transmission Electron Micrograph of Ti-4Al Strained Approximately 10%	47
29	Transmission Electron Micrograph of Ti-4Al Strained Approximately 10%	48
30	Transmission Electron Micrograph of Ti-8Al Deformed Approximately 10%	49
31	Transmission Electron Micrograph of Ti-8Al-1Mo-1V Duplex Annealed, Strained Approximately 15%	50
32	Transmission Electron Micrograph of Ti-8Al-1Mo-1V Duplex Annealed Strained Approximately 15%	51
33	Transmission Electron Micrograph of Ti-8Al-1Mo-1V Solution Annealed at 2000°F, Air Quenched	52
34	Transmission Electron Micrograph of Ti-8Al-1Mo-1V Solution Annealed at 2000°F, Air Quenched, Strained Approximately 5%	53
35	Transmission Electron Micrograph of Ti-8Al-1Mo-1V Solution Annealed at 2000°F, Air Quenched, Strained Approximately 8%	54
36	Transmission Electron Micrograph of Ti-8Al-1Mo-1V Solution Annealed at 2000°F, Air Quenched, Deformed Approximately 8%	55

TABLES

I	Effect of Heating at Different Test Temperatures on the Stress Intensity Factor for Ti-8Al-1Mo-1V in 3% NaCl Solution	7
II	Effect of Hydrogen on Stress Intensity Factor for Ti-8Al-1Mo-1V Alloy in 3% NaCl Solution	10
III	Effect of Heat Treatment Variables on the Stress Intensity Factor for Ti-8Al-1Mo-1V in 3% NaCl Solution	14
IV	Concentration of Added Tritium in Ti-8Al-1Mo-1V in 1800°F Solution Annealed and Aged Condition	20
V	Mechanical Properties of Titanium-Aluminum Alpha Alloys	35
VI	Effect of Aluminum Content on Stress Corrosion of Alpha Titanium	36

1.0 INTRODUCTION

The commercial alpha-beta alloys have received widespread attention as candidate structural materials for the supersonic transport aircraft because of their high strength and weldability.⁽¹⁾ They are being extensively evaluated in new types of environments because of the need for long time service assurance as tankage materials that are not subject to sudden failure such as stress corrosion cracking (SCC).

Many investigations have been conducted to determine the particular factors that make an alloy susceptible to stress corrosion cracking (SCC) in a specific environment. The variety of factors suggested have included pre-existing susceptible paths, anodic or cathodic active precipitates, low stacking fault energy lattice, co-planar arrays of dislocations, short range ordering, rupture of passive films, aqueous complex compound formation chemisorption of ions, formation of active hydrides and segregation of interstitial or substitutional solute atoms to dislocations.

In general, it has been recognized that what may distinguish a susceptible alloy from a nonsusceptible alloy to transgranular SCC are: (1) it must develop wide slip when plastically deformed, (2) must rupture the passive surface film, and (3) be exposed to an environment in which some part of a large active slip step surface is not partially repassivated within a critical time period.⁽²⁾

The Astropower Laboratory is engaged in a program of NASA sponsored research to develop fundamental knowledge about the mechanism of SCC of titanium alloys in aqueous solutions. Study of the behavior of alpha type and alpha-beta type alloys is emphasized, because they are known to exhibit susceptibility to SCC and are candidate materials for tankage and supersonic transport applications. The results obtained from the previous investigation are presented in detail in Yearly Summary Report SM-49105-F1⁽³⁾ and briefly are summarized below.

- (a) Precracked notched alpha type Ti-5Al-2.5Sn and alpha-beta type Ti-8Al-1Mo-1V alloys exhibited high sensitivity to crack propagation in distilled water and in 3% NaCl solutions, whereas alpha-beta type Ti-6Al-4V was less sensitive to 3% NaCl solution, and did not exhibit noticeable effect in distilled water.

- (b) Alpha and alpha-beta type alloys exhibit mixtures of ductile dimple and brittle cleavage areas in fracture faces. The cleavage areas are much larger in SCC in aqueous salt solutions, compared to SCC in distilled water. The stress corrosion paths propagate transgranularly through alpha grains, but appear to follow by cleavage at the alpha-beta boundaries.
- (c) Electron microautoradiography studies clearly demonstrated that hydrogen gas in quantities less than 50 ppm (in radiotracer form A3) introduced into titanium alloys is preferentially segregated in beta phase in alpha-beta type alloys, and is uniformly dispersed in all beta type alloys. The concentration of hydrogen in the beta phase of alpha-beta alloys containing approximately 40 ppm was estimated to vary from 160 ppm for Ti-6Al-4V, and approximately 250 ppm for Ti-8Al-1Mo-1V, and Ti-5Al-2.5 Sn alloys.
- (d) High stress concentration around crack tips does not appear to cause hydrogen segregation or change in hydrogen distribution between the alpha phase matrix and beta phase particles in alpha-beta alloys.

The presence of hydrogen-bearing compounds in most, if not all, environments is known to cause deleterious effects on the mechanical properties of titanium alloys, but the nature of such effects in SCC is not well known. The primary object of our studies is to elucidate the role of hydrogen in SCC of titanium alloys in aqueous environments. Studies were conducted to elucidate the effect of different total hydrogen content and the change in hydrogen segregation by various solution treatments on SCC. Also, attempts were made to assess the effect of aluminum content on the susceptibility to SCC.

2.0 EXPERIMENTAL EVALUATIONS

2.1 Effect of Microstructure and Hydrogen Content on Susceptibility to Stress Corrosion Cracking (SCC)

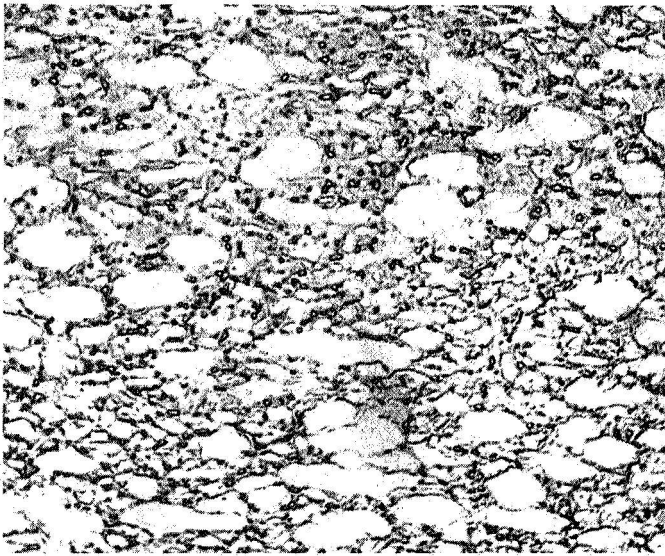
Susceptibility to SCC is of great importance. A large change in fracture strength of Ti-8Al-1Mo-1V alloy in aqueous KCl with solution treatment between 900°C to 1000°C was shown by Beck.⁽⁴⁾ Curtis and Spurr⁽⁵⁾ demonstrated that elimination of large, equiaxed alpha grains in Ti-6Al-4V by treatment in the beta-phase field prior to aging improves both fracture toughness and stress corrosion resistance. Material rolled within 50°F of the beta transus exhibits the optimum properties characteristic of the acicular morphology.

In the present program, attempts were made to evaluate the effect of total hydrogen content and hydrogen distribution in alpha-beta alloy on susceptibility to SCC.

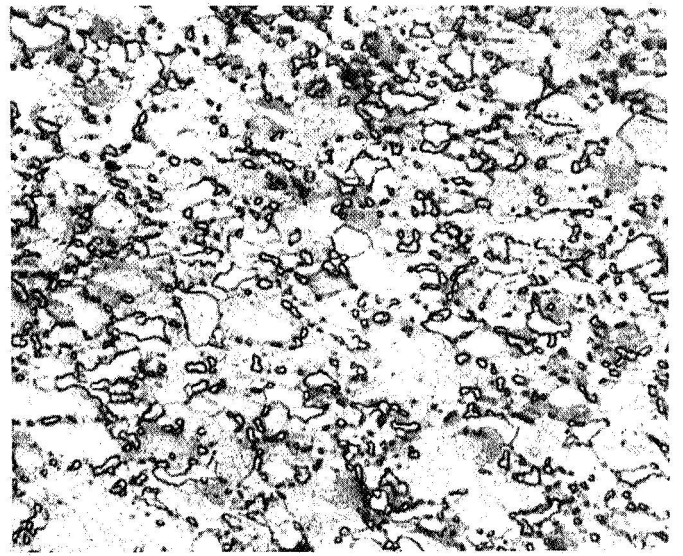
Different amounts of hydrogen from 10 ppm to 100 ppm were introduced into the Ti-8Al-1Mo-1V alloy, and the change in susceptibility to SCC in aqueous salt environments was determined by examining the change in stress intensity factor. The relation of hydrogen segregation in beta phase for different solution treatments at 1600°F and 1800°F, and also in acicular structures produced by rapid quenching from above the beta transus in alpha-beta alloy Ti-8Al-1Mo-1V, was determined by microautoradiography. These experiments are designed to clearly establish whether there are different threshold values of hydrogen for resistance to SCC cracking and how this is related to the capability of beta phase of different composition and heat treat condition to absorb and retain hydrogen.

Sheet material of Ti-8Al-1Mo-1V obtained from Titanium Metals Corporation was 0.109" in thickness; the composition and mechanical properties were previously reported.⁽³⁾

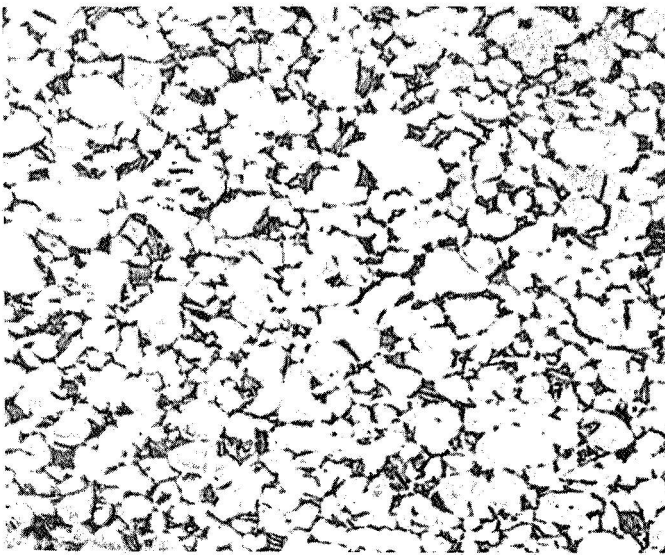
Heat treatments of Ti-8Al-1Mo-1V have been made at 1600°F, 1800°F, and heat treatments were conducted in vacuum in quartz tubes employing 10^{-4} or 10^{-6} torr. The microstructure of the as-received material and different vacuum heat treatments are shown in Figure 1.



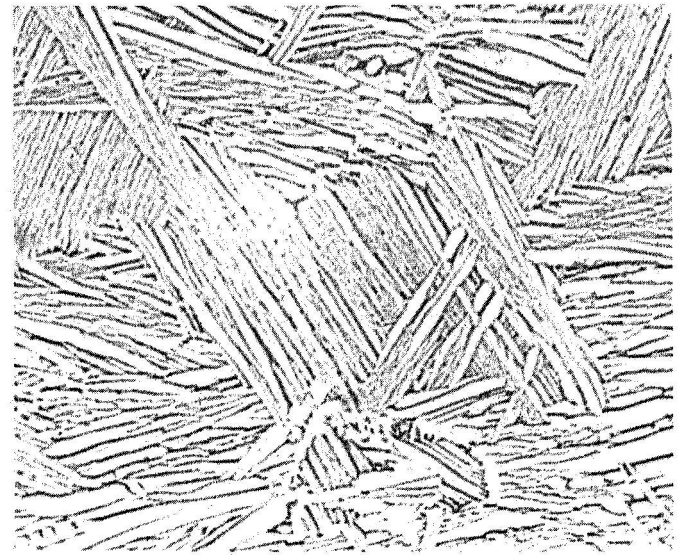
a



b



c



d

- (a) As-received
- (b) 1600°F Solution Heat Treatment, Air Quench
- (c) 1800°F Solution Heat Treatment, Air Quench
- (d) 2000°F Solution Heat Treatment, Air Quench

c367

Figure 1. Microstructure of Ti-8Al-1Mo-1V Following Different Solution Heat Treatments. Etch: Kellers Reagent (600X Reduced 23% for Printing)

Hydrogen was introduced into specimens of Ti-8Al-1Mo-1V at 1600°F and 1800°F by gas absorption employing a modified Sieverts apparatus previously described.⁽³⁾ In order to charge the titanium alloy, the quartz tubes containing an alloy sample were evacuated to 10^{-7} torr and heated to 1350°F ± 10°F and held at this temperature until degassing was completed in about 1/2 hour. The specimen tube was cooled to ambient temperature, research grade hydrogen was added to the tube, the tube was reheated to the solution heat treat temperature, and held at temperature for 1/2 hour. The specimen tube was then cooled to ambient temperature and the final pressure was measured. The amount of hydrogen introduced into each alloy heat treatment was estimated from the pressure drop.

Stress corrosion tests were conducted by loading single-edge-notched specimens in a Dillon tensile machine. The load was measured with a Baldwin-Lima-Hamilton SR-4 Load Cell which is capable of measuring the total load within four pounds. The corrosion solution is contained in a lucite box sealed to the specimen with an epoxy to prevent leakage. 3% NaCl solution at ambient temperature was the corrosion solution. Crack extension was observed with a stereomicroscope. The initial specimen for each alloy heat treatment was loaded and held for five minutes. Eventually a load was reached that caused the specimen to fracture. The time-to-fracture was measured with a stopwatch. The initial stress intensity factor, K_{Ii} , was calculated using the load that caused crack propagation to start. For single-edge-notched specimen, the stress intensity factor, K , was calculated from the expression recommended by Srawley and Brown.⁽⁶⁾

$$K = \frac{Pa}{Bw} \left[1.99 - 0.41 \frac{a}{w} + 18.70 \left(\frac{a}{w}\right)^2 - 38.48 \left(\frac{a}{w}\right)^3 + 58.85 \left(\frac{a}{w}\right)^4 \right]$$

where

P = load

B = thickness

a = crack length

w = width

For each specimen, the initial crack length, a , was measured with a low power microscope following fracture of the specimen, and was used to calculate K_{Ii} .

From the results obtained with the initial specimen, load levels were selected for stressing each alloy. The initial stress intensity factor, K_{Ii} , to propagate a crack in 3% salt solution for Ti-8Al-1Mo-1V at 1600°F, 1800°F, and 2000°F solution heat treatments is shown in Table I. A comparison of the initial stress intensity factor, K_{Ii} , in 3% salt solution at ambient temperature with values of K_{Ic} obtained in air showed that Ti-8Al-1Mo-1V in the as-received duplex annealed condition and solution heat treated at 1600°F and 1700°F was susceptible to SCC. Ti-8Al-1Mo-1V solution heat treated at 1800°F or 2000°F, was immune to SCC.

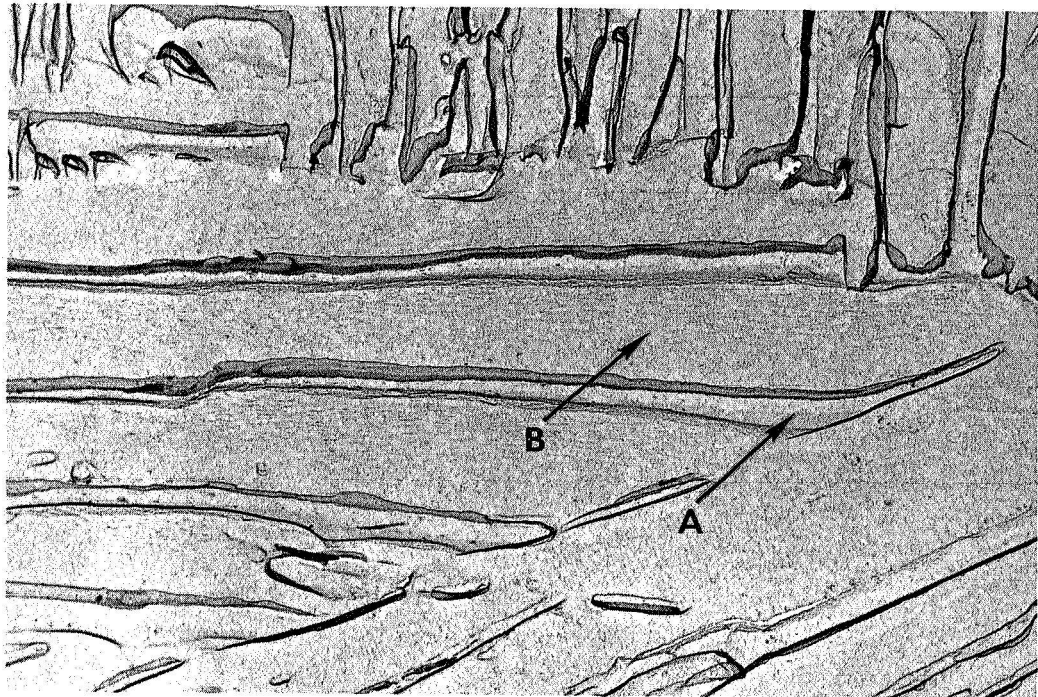
Air quenching from temperatures of 1800°F or above produces acicular martensitic structures, the higher the temperature, the higher the amount of acicular structure. The morphology of the solution-treated samples that exhibited immunity to SCC was examined under higher magnification in the electron microscope (see Figures 2 and 3). At temperatures above the beta transus (2000°F) the entire structure is acicular, consisting of retained beta and martensitic alpha lamella (see Figure 2). At 1800°F solution-annealing the acicular structure of beta plus martensitic alpha is distributed in islands near the grain boundaries of the equiaxed alpha matrix (see Figure 3).

The microstructural changes produced by different solution treatments of Ti-8Al-1Mo-1V can be observed and are associated with susceptibility to SCC. However, whether alloying elements and interstitial elements can migrate during phase transformations, and thus affect susceptibility to SCC, is not known and cannot be detected by direct microscopic examination.

In the present program, attempts were made to introduce different amounts of total hydrogen from 10 to 100 ppm into the Ti-8Al-1Mo-1V alloy and examine hydrogen microsegregation into different phases and its effect on the initial stress intensity factor, K_{Ii} , in aqueous salt environments. The results are shown in Table II.

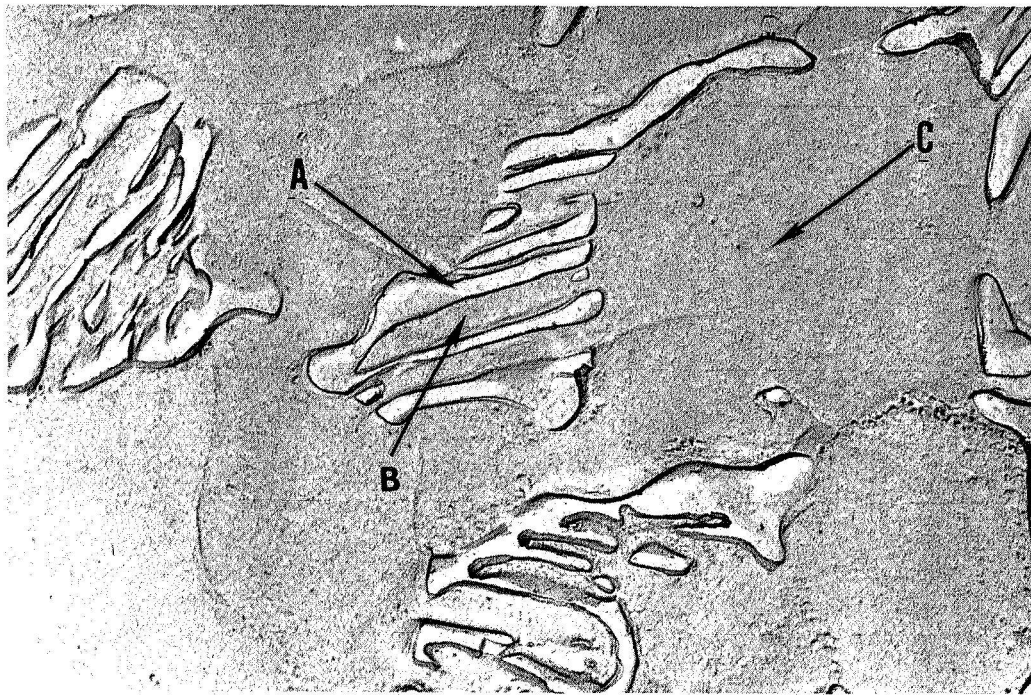
TABLE I
EFFECT OF HEATING AT DIFFERENT TEST TEMPERATURES
ON THE STRESS INTENSITY FACTOR FOR
Ti-8Al-1Mo-1V in 3% NaCl SOLUTION

<u>Heat Treatment</u>	<u>Environment</u>	<u>Hydrogen Content</u>	K_{Ii} ksi $\sqrt{\text{in.}}$	<u>Time to Fracture</u>
As received in Duplex Annealed	Argon	36	43.7	---
	Argon	36	44.8	---
	3% NaCl	36	28.0	0.6
	" "	36	25.2	1.0
	" "	36	23.0	1.0
	" "	36	18.5	1.5
1600°F, 2 hrs, AQ (vacuum 10 ⁻⁶ torr)	Air	27	78	---
	3% NaCl	27	20.2	5.0
	" "	27	21.2	3.0
	" "	27	27.0	4.0
1700°F, 24 hrs, AQ (vacuum 10 ⁻⁶ torr)	Air	23	82.0	---
	3% NaCl	23	30.0	3.5
	" "	23	32.0	2.0
1800°F, 2 hrs, AQ (vacuum 10 ⁻⁶ torr)	Air	25	87.2	---
	3% NaCl	25	84.0	---
2000°F, 1 hr, AQ (vacuum 10 ⁻⁴)	Air	27	70.6	---
	3% NaCl	27	74.0	---
2000°F, 2 hrs, AQ	Air	14	87.0	---
	3% NaCl	14	86.8	---



c3851

Figure 2. Electron Micrograph Illustrating the Fine Details of the Acicular Structure Shown in Figure 1d. Note (A) is retained beta, and (B) is martensitic alpha lamella. Magnification 11,500X



c3852

Figure 3. Electron Micrographs Illustrating the Islands of Acicular Structure of Retained Beta (A) and Martensitic Alpha (B) in Equiaxed Alpha Matrix (C) as in Figure 1c. Magnification 11,500X

TABLE II

EFFECT OF HYDROGEN ON STRESS INTENSITY FACTOR FOR
Ti-8Al-1Mo-1V ALLOY IN 3% NaCl SOLUTION

<u>Heat Treatment</u>	<u>Environment</u>	<u>Hydrogen Content ppm</u>	<u>K_{Ii} ksi $\sqrt{in.}$</u>	<u>Time to Fracture (min)</u>
1600 ^o F, 2 hrs, AQ	Air	27	78	---
	3% NaCl	"	20.2	5.0
	" "	"	27.0	3.0
	" "	"	27.0	4.0
1600 ^o F, 1 hr, AQ	Air	110	61.7	---
	3% NaCl	"	19.4	3.5
	" "	"	18.4	2.5
	" "	"	16.6	4.5
1800 ^o F, 2 hrs, AQ	Air	25	87.2	---
	3% NaCl	"	84.0	---
1800 ^o F, 1 hr, AQ	Air	100	83.0	---
	3% NaCl	"	80.2	---
	" "	"	86.0	---

For heat treatment of Ti-8Al-1Mo-1V at 1600°F in which 110 ppm of hydrogen was charged into the alloy, the value of initial stress intensity factor was plotted versus the time for fracture in Figure 4. An examination of the curve shows a minimum value of 16 ksi $\sqrt{\text{in.}}$ below which no stress corrosion failure is observed. This is designated K_{Isc} after Brown.⁽⁷⁾ Ti-8Al-1Mo-1V solution heat at 1800°F was immune to SCC with hydrogen contents as high as 100 ppm.

The martensite that forms at 1800°F or higher temperatures has a hexagonal structure⁽⁸⁾ and is immune to SCC. Reheating structures with a 1800°F martensitic phase through 1450°F causes partial spheroidization (A) of retained beta needles (see Figure 5) and decomposition of martensitic alpha. Fracture toughness specimens which had been solution annealed at 1800°F, followed by air quenching were heated at 900°F and 1450°F in a vacuum atmosphere, 10^{-6} torr. The results are shown in Table III. The initial specimens were step loaded, starting at a stress intensity factor of 30 ksi $\sqrt{\text{in.}}$ and the load was increased every five minutes. No susceptibility was observed for this specimen; however, when the initial load was increased SCC was observed. For this heat treatment, SCC apparently is related to the strain rate at crack tip.

2.2 Microautoradiography Studies

It has been previously pointed out that hydrogen may preferentially segregate into beta phase particles or at the alpha-beta phase boundaries in alpha-plus-beta phase alloy structures.⁽¹⁾ Attempts were made in the present program to evaluate the partition of hydrogen between alpha and beta phases by using tritium and electron microautoradiography technique.

Specimens of Ti-8Al-1Mo-1V that had an initial hydrogen concentration of 10 ppm, produced by vacuum solution-heat treatment of 2000°F for two hours, were air quenched and solution annealed at 1600°F for two hours. Carrier-free tritium was charged into the specimens at two concentrations — one at 13 ppm, and the other at 40 ppm.

The electron microautoradiographs of the specimens were prepared as follows:

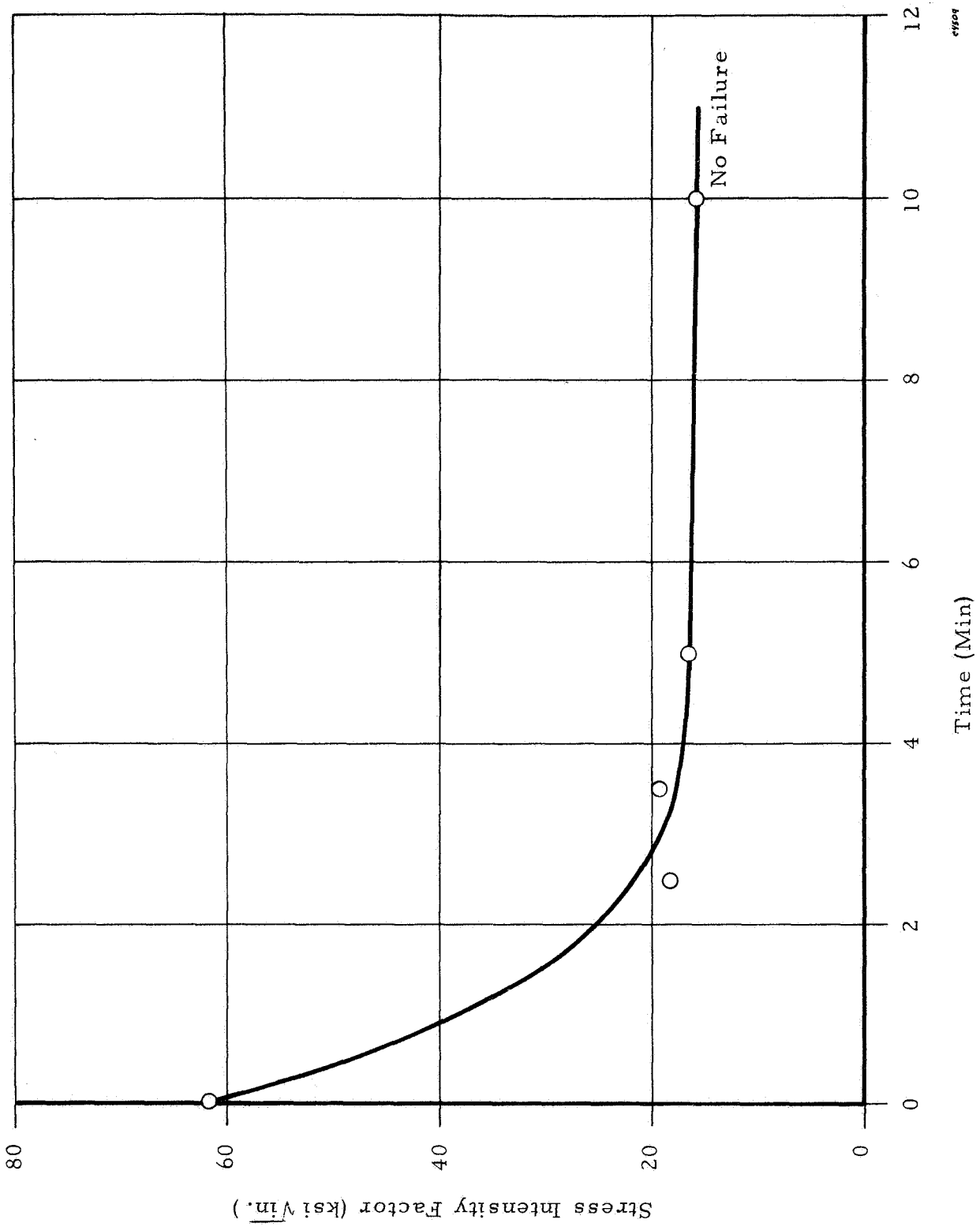


Figure 4. Effect of Stress Intensity on Time-to-Fracture for Ti-8Al-1Mo-1V, 1600°F Heat Treatment with 110 ppm Added H₂ in 3% NaCl Solution



03807

Figure 5. Electron Micrograph of Alloy Sample Solution-Annealed at 1800°F and Aged at 1450°F. Note partial spheroidization of beta particles. Magnification 4000X

TABLE III
EFFECT OF HEAT TREATMENT VARIABLES
ON THE STRESS INTENSITY FACTOR FOR
Ti-8Al-1Mo-1V in 3% NaCl SOLUTION

<u>Heat Treatment</u>	<u>Environment</u>	<u>Hydrogen Content</u>	K_{Ii} <u>ksi $\sqrt{\text{in.}}$</u>	<u>Time to Fracture (min)</u>
1800°F, 2 hrs, AQ	Air	14	78.2	---
+ 1450°F, 8 hrs, AQ	3% NaCl	14	77.6*	---
	" "	14	83.0*	---
	" "	14	47.3	3.0
	" "	14	38.7	5.0
	Air	100	66.6	---
	3% NaCl	100	30.4	2.0
1800°F, 2 hrs, AQ	Air	23	86.7	---
+ 900°F, 300 hrs, AQ	3% NaCl	23	42.0	1.5
	" "	23	33.6	3.0
	" "	23	25.1	4.0
2000°F, 2 hrs, AQ	Air	10	84.5	---
+ 1600°F, 2 hrs, AQ	3% NaCl	10	34.6	4.0
	" "	10	34.0	9.0

*Step Loaded

1. The specimens were lightly polished and ten angstroms of Cr were deposited to act as a shadow, and 150 angstroms of carbon were deposited for direct replica onto the polished surface.
2. The specimens were transferred to the darkroom, and a monolayer of Kodak NTE nuclear track emulsion was then placed on the surface, and the specimens were exposed for 16 hours.
3. The emulsion was developed while on the specimen and fixed.
4. Three layers of 5% Parlodian were placed on the surface and allowed to dry, and electron microscope grids were placed in the fourth layer.
5. Parlodian plus emulsion was mechanically stripped from the surface, and the Parlodian substrate dissolved in amyl acetate.

Figures 6 and 7 show microautoradiographs of the specimens containing 13 ppm and 40 ppm of tritium. The tritium was quite evenly distributed in the alloy at 13 ppm concentration. It was concentrated in the beta phase and at the alpha-beta interfaces at 40 ppm concentration.

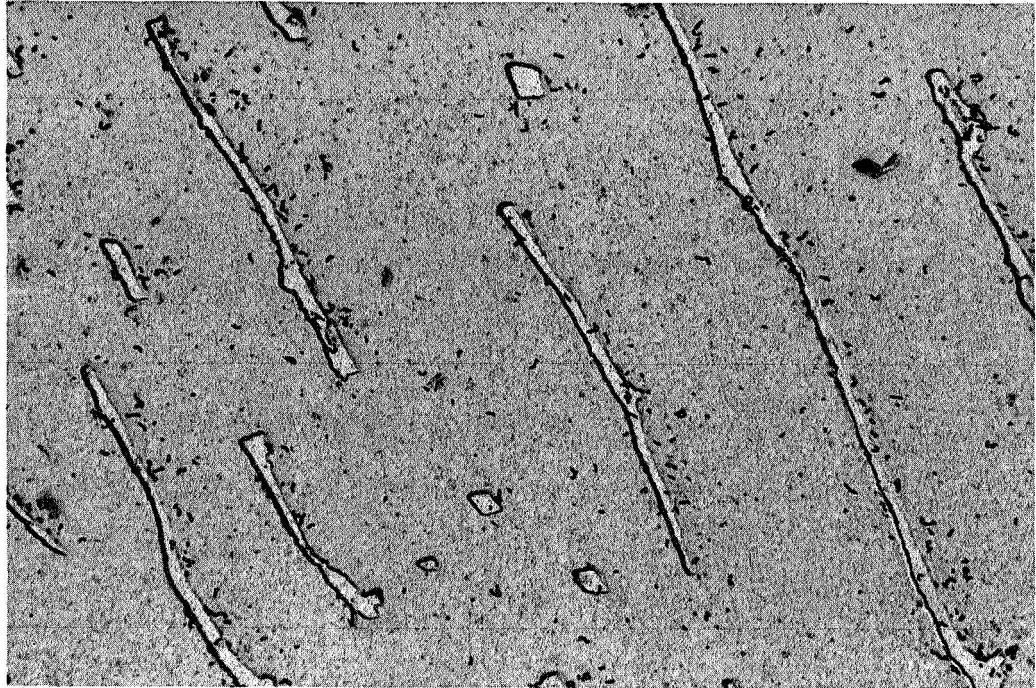
In order to estimate tritium concentration in the beta phase particles, it was necessary to determine the emulsion recording efficiency from the expression $\frac{\text{filaments/cm}^2 \text{ observed}}{\text{beta particles reaching surface}}$. For this purpose a uniform tritium distribution was obtained by charging an all-alpha Ti-3.1Al specimen with 42 ppm of tritium, and the number of filaments per cm² observed were counted. (See Figure 8.) The emulsion recording efficiency was calculated by a method previously described. ⁽³⁾

The total fraction of beta radiation reaching the emulsion surface will be the fraction being transmitted after self absorption multiplied by fraction obtained from geometry distribution considerations

$$F = 0.36 \times 0.364 = 0.131$$

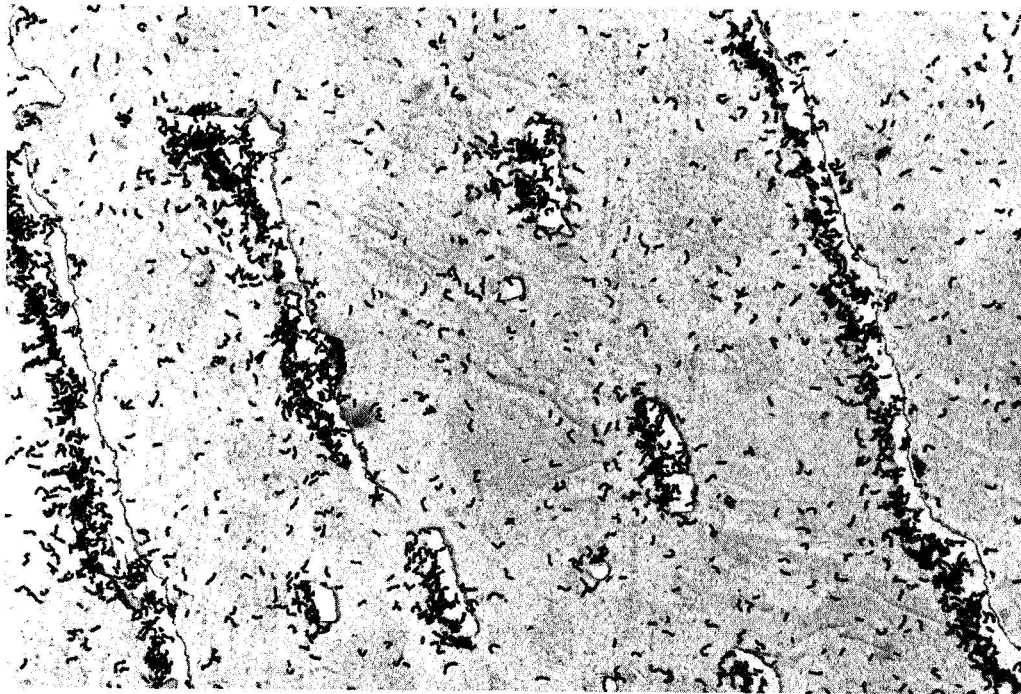
The volume of the alloy contributing to each square cm of emulsion is $1.8 \times 10^{-5} \times 1 \text{ cm}^2$. The total number of tritium (H^3) atoms present in this volume which contains 42 ppm carrier free tritium by weight is

$$N = \frac{1.8 \times 10^{-5} \times 4.46}{3} \times 42 \times 10^{-6} \times 6.02 \times 10^{23} = 6.7 \times 10^{14}$$



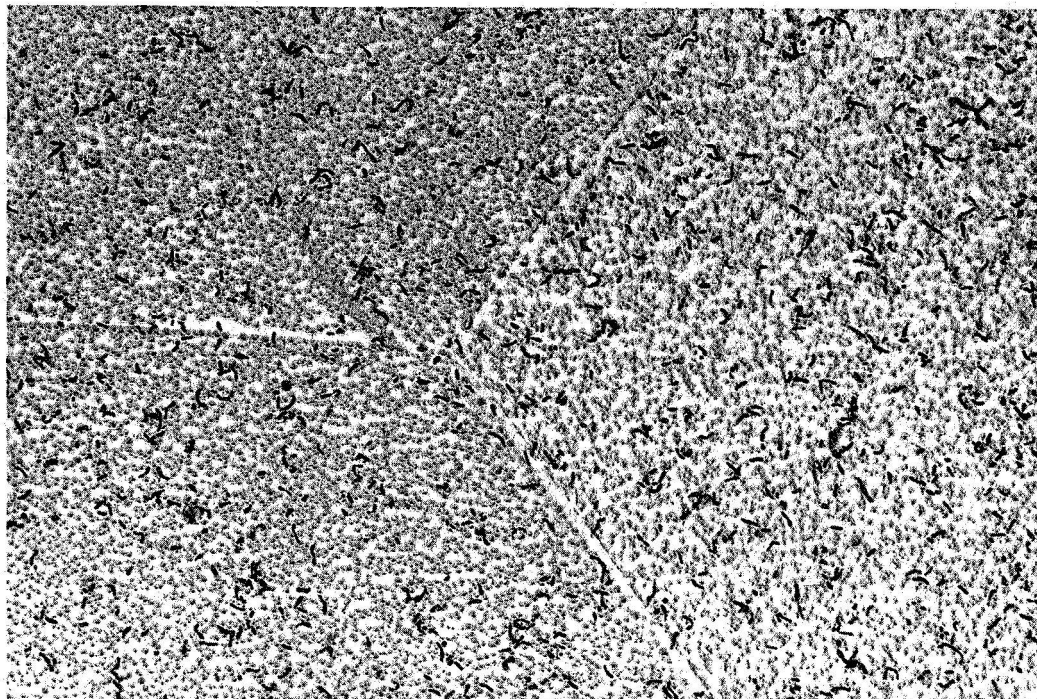
03855

Figure 6. Microautoradiograph of Tritium in Ti-8Al-1Mo-1V, 2000°F, 2 Hours, A.Q. + 1600°F, 2 Hours, A.Q. Containing 13 ppm. Magnification 11,500X



c3056

Figure 7. Microautoradiograph of Tritium in Ti-8Al-1Mo-1V, 2000°F, 2 Hours, A. Q. + 1600°F, 2 Hours, A. Q. Containing 40 ppm. Tritium is highly concentrated in beta phase and at alpha-beta boundaries. Magnification 11,500X



•3857

Figure 8. Microautoradiograph of Tritium in Ti-3.1Al.
Magnification 28,000X

The number of beta particles or disintegrations from the long half-life tritium nuclei can be calculated from the expression

$$N_0 - N = N_0 \lambda t$$

t = disintegration or exposure time, 16 hours

$$\lambda = \text{disintegration constant} = \frac{0.643}{t_{1/2}} = 6.3 \times 10^{-6} \text{ hrs}^{-1} = 1.82 \times 10^{-9} \text{ sec}^{-1}$$

$$\begin{aligned} N_0 - N &= 6.7 \times 10^{14} \times 1.82 \times 10^{-9} \times 16 \times 3600 \\ &= 7.02 \times 10^{10} \end{aligned}$$

The amount of beta particles reaching the emulsion surface is therefore

$$7.02 \times 10^{10} \times 0.131 = 9.2 \times 10^9$$

The emulsion efficiency estimated from Ti-3.1Al microautoradiographs is therefore

$$\frac{\text{filaments/cm}^2 \text{ observed}}{\text{beta particles reaching surface}} = \frac{29.4 \times 10^8 \times 100}{9.2 \times 10^9} = 32$$

The specimens shown in Figures 6 and 7 contained approximately 8% beta phase. The specimen with 10 ppm total tritium content had a tritium concentration of about 20/10 ratio in the beta phase, and the specimen with 40 ppm total tritium content had a tritium concentration of about 300/15 ratio in the beta phase.

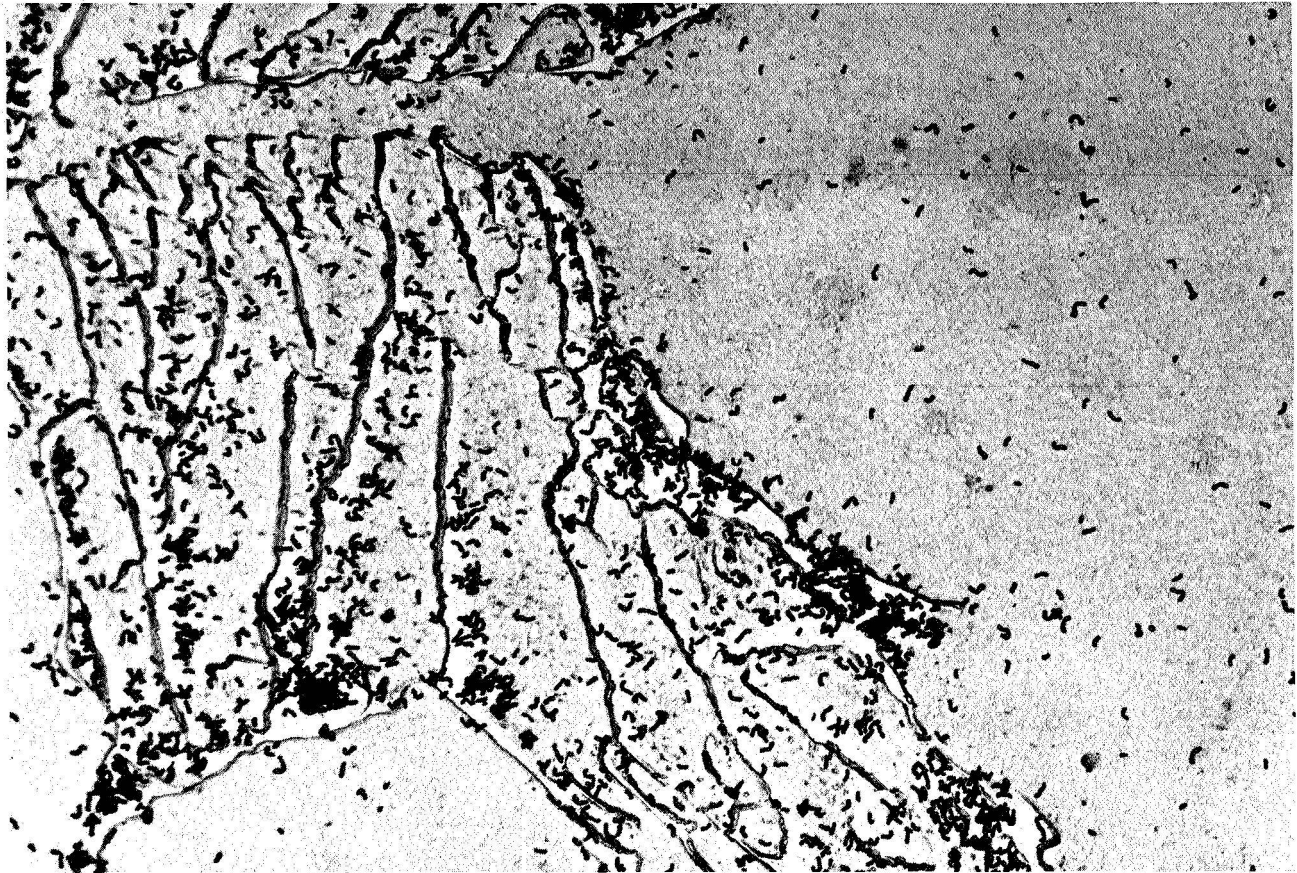
The hydrogen distribution was studied in Ti-8Al-1Mo-1V solution heat treat 1800°F, 2 hours, AQ and solution heat treat 1800°F plus aging at 1450°F and 900°F. The heat treatment plus tritium charging conditions are shown in Table IV.

Figure 9 shows a microautoradiograph of tritium charged at 1860°F, 30 min, AQ. When the alloy exhibits script type islands of plate-like martensitic alpha and beta in equiaxed alpha matrix by 1800°F solution annealing, hydrogen concentrates in alpha-beta grain boundary regions or in

TABLE IV

CONCENTRATION OF ADDED TRITIUM IN
Ti-8Al-1Mo-1V IN 1800°F SOLUTION
ANNEALED AND AGED CONDITION

Heat Treatment	Tritium Changing Temperature	Tritium
1800°F, 30 min, AQ	1860°F	40
1800°F, 2 hrs, AQ + 1450°F, 6 hrs, AQ	1450°F	37
1800°F, 2 hrs, AQ + 900°F, 18 hrs, AQ	900°F	60



03808

Figure 9. Electron Microautoradiograph of Ti-8Al-1Mo-1V Alloy Containing 40 ppm Tritium in 1800°F Solution Annealed Condition. Note concentration of tritium in alpha-beta boundaries and in beta-martensitic alpha regions. Magnification 11,500X

the plate-like beta-grain boundary regions or in the plate-like beta- martensitic alpha islands rather than in the equiaxed alpha.

Figure 10 shows microautoradiograph of tritium in 1800°F solution annealed Ti-8Al-1Mo-1V plus a 1450°F stabilization anneal. Tritium is concentrated in spherodized beta. Figure 11 shows a microautoradiograph of tritium in 1800°F solution anneal plus aging at 900°F. The tritium is concentrated in acicular islands. The retained beta structure cannot be resolved in this microautoradiograph.

Single-edge notch specimens of Ti-8Al-1Mo-1V duplex annealed and 1600°F solution heat treated were stress corrosion cracked in tritiated water and 3% NaCl tritiated aqueous solution. The fracture surfaces were examined by microautoradiography for evidence of absorption of elemental tritium generated during SCC.

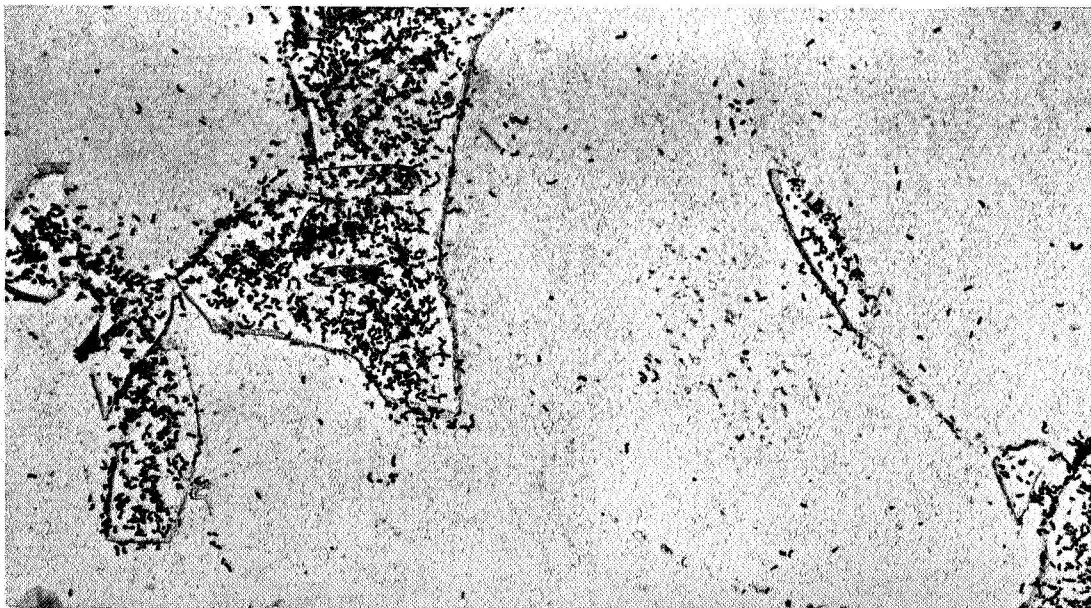
The tritiated water solution was prepared by diluting 1 curie/cc tritiated water with 50 cc of distilled water. One specimen of Ti-8Al-1Mo-1V was stress corrosion cracked at an initial stress intensity, (K_{II}) of 28 ksi $\sqrt{\text{in.}}$ in 10 cc of this solution. NaCl was added to the remaining tritiated water to make a 3% salt solution. One single-edge fracture toughness specimen of Ti-8Al-1Mo-1V duplex annealed was stress corrosion cracked in 10 cc of 3% NaCl tritiated aqueous solution at an initial stress intensity of 16.5 ksi $\sqrt{\text{in.}}$ One single-edge notch specimen of Ti-8Al-1Mo-1V solution heat treated at 1600°F was stress corrosion cracked at a stress intensity of 25 ksi $\sqrt{\text{in.}}$ All of the fractured surfaces were rinsed in flowing distilled water for ten minutes to remove tritiated water which might adsorb on the freshly cleaved surfaces prior to making autoradiographs.

The procedures for making microautoradiographs on fractured surfaces are very similar for polished surfaces. The electron microautoradiographs of the specimens were prepared as follows:

1. Ten angstroms of Cr were deposited on fractured specimens to act as a shadow, and 150 angstroms of carbon were deposited for direct replica on Cr.
2. The specimens were transferred to the darkroom, and a layer of Kodak NTE nuclear track emulsion was then placed on the surface, and the specimens

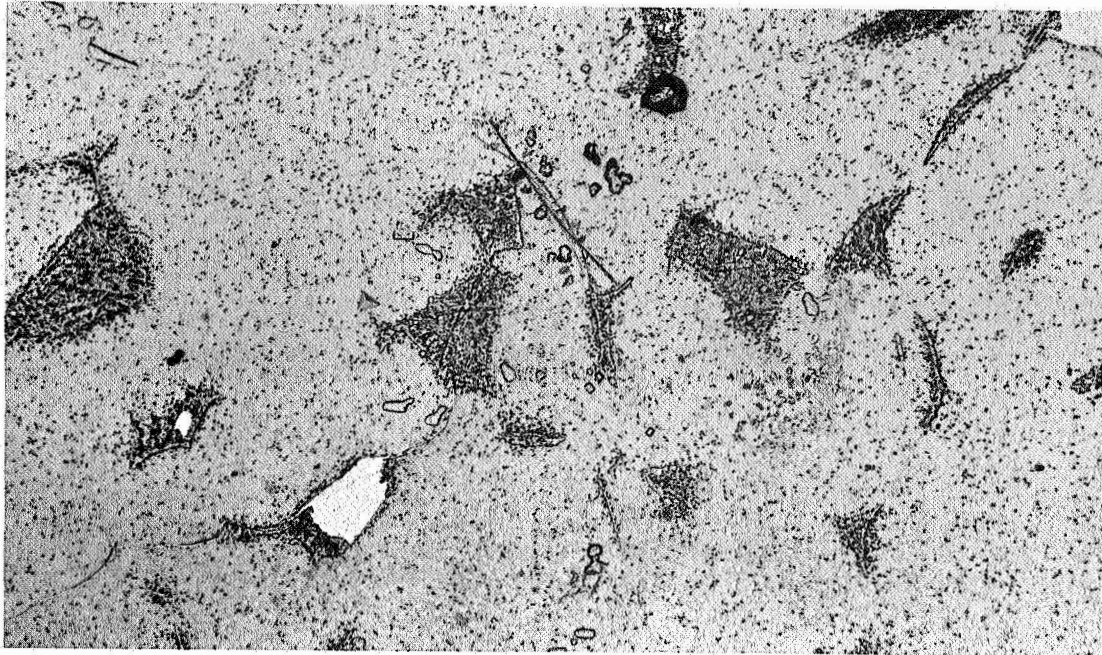


Magnification 4000X

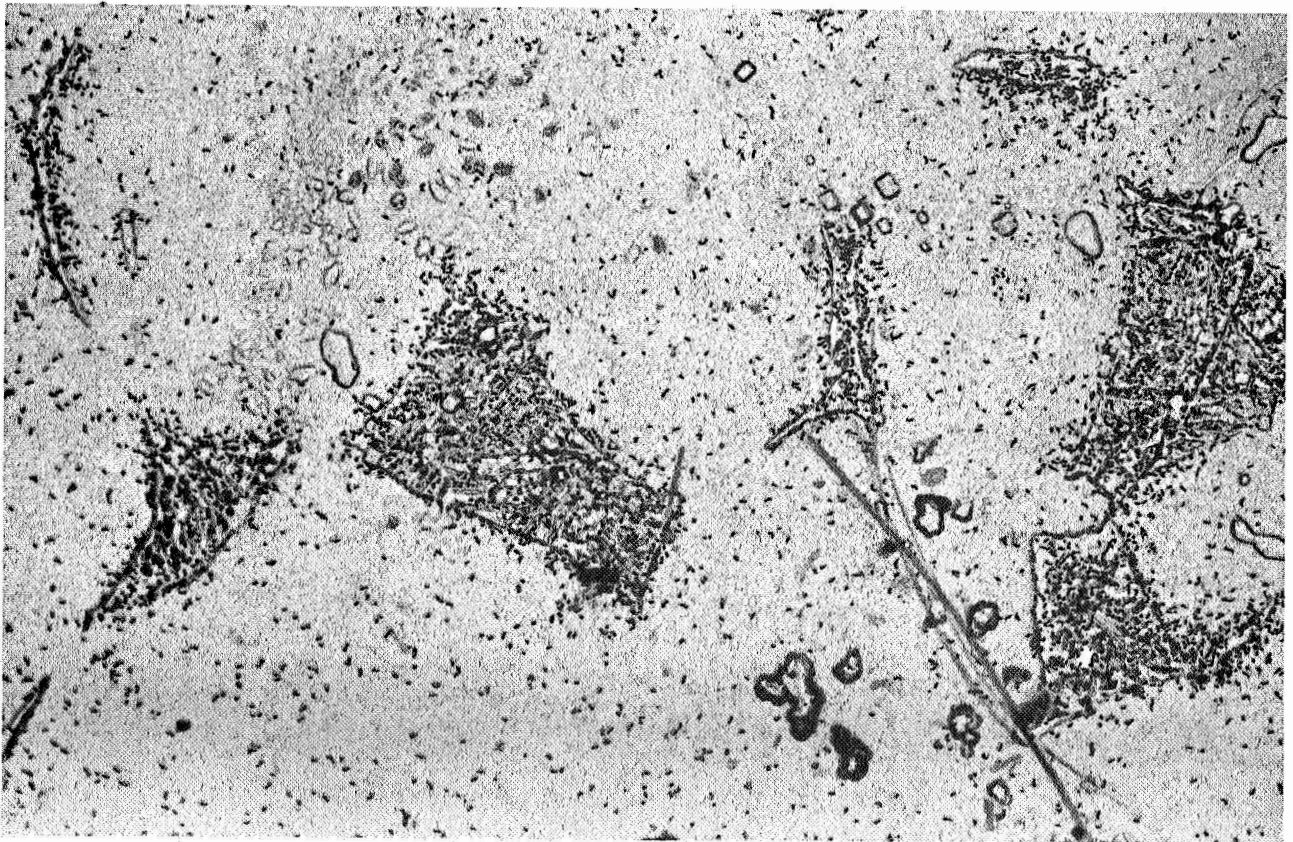


Magnification 11000X

Figure 10. Electron Microautoradiograph of Tritium in Ti-8Al-1Mo-1V Alloy Solution Annealed at 1800°F and Stabilized at 1450°F, Then Tritium Charged at 1450°F. Note tritium is concentrated in spheroidized beta.



Magnification 4000X



Magnification 11000X

Figure 11. Electron Microautoradiograph of Tritium in Ti-8Al-1Mo-1V Alloy Solution Annealed at 1800°F and Aged at 900°F, Then Tritium Charged at 900°F. Note, the tritium is concentrated in acicular martensitic islands.

were exposed for 16 hours. Due to the roughness of fractured surfaces probably more than a monolayer of emulsion accumulated in crevice areas.

3. The emulsion was developed while on the specimen and fixed.
4. Five percent Parlodion was placed on the surface and allowed to dry.
5. Parlodion plus emulsion was mechanically stripped from the surface.
6. An additional layer of carbon was deposited on stripped surface to strengthen the replica.
7. The Parlodion was dissolved in amyl acetate.

A single-edge notch specimen of Ti-6Al-4V which had been previously charged with 30 ppm tritium was fractured in air and used to check the technique described above. A microautoradiograph of the fractured surface is shown in Figure 12. The tritium segregation in the beta phase is clearly seen.

Figures 13 and 14 show microautoradiographs of fractured surfaces of single-edge notch specimens of Ti-8Al-1Mo-1V (duplex annealed) which were stress corrosion cracked in distilled water and 3% NaCl, respectively. Figure 15 shows a microautoradiograph of a fractured surface Ti-8Al-1Mo-1V, solution heat-treated at 1600°F, 2 hours, AQ, fractured in 3% NaCl.

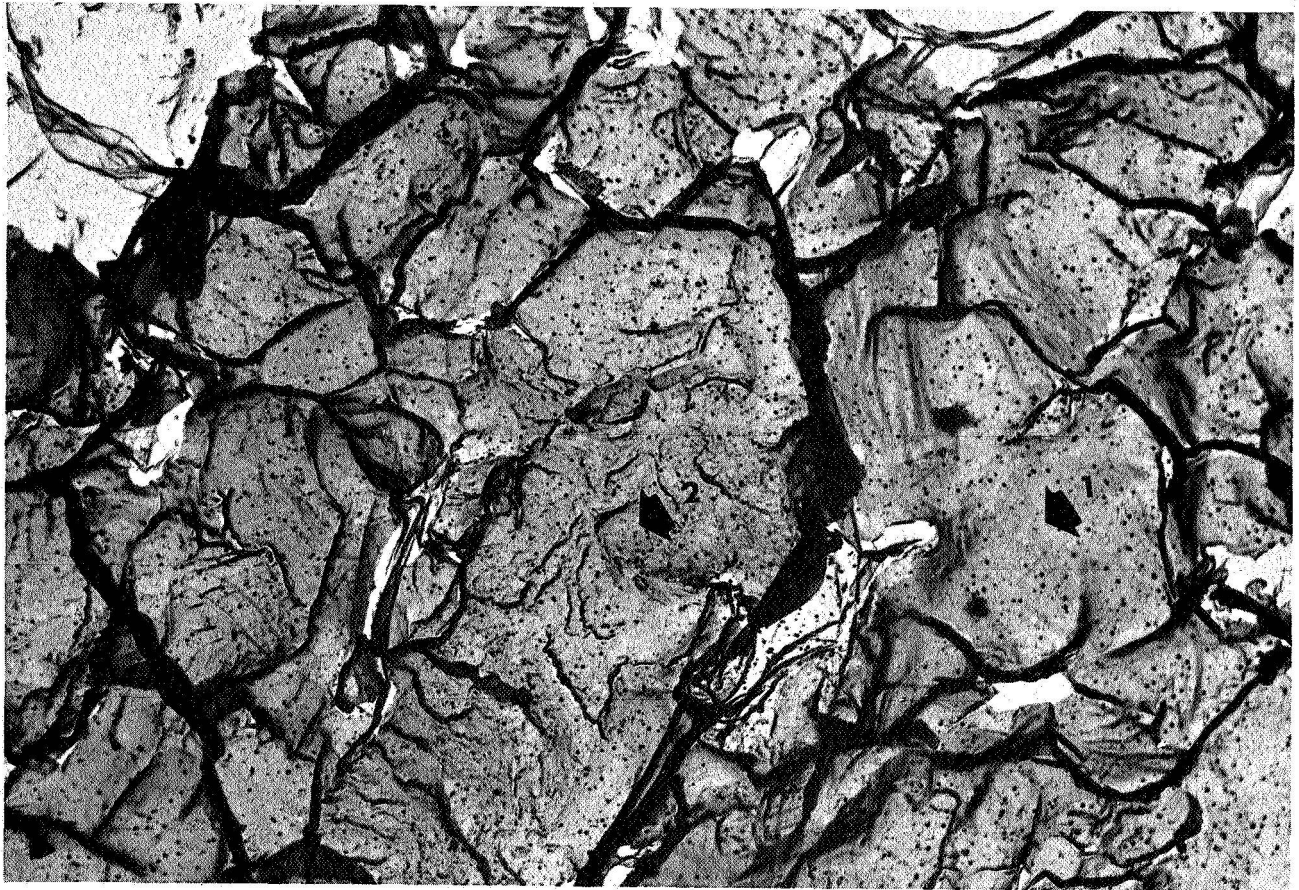
These specimens of Ti-8Al-1Mo-1V alloy stress corrosion cracked in distilled water with 2% tritiated water and in 3% NaCl solution with 2% tritiated water did not appear to exhibit evidence of hydrogen (tritium) diffusion into the fractured face by electron microautoradiography. If the alloy sample had retained tritium below the surface layer, it would have been easily detected by this technique.

Single-edge notch specimens of Ti-8Al, Ti-8Al-1Mo-1V and Ti-5Al-2.5Sn were charged with approximately 30 ppm of tritium at 1450°F. These specimens were fractured in 3% NaCl solution at ambient temperature. Electron microautoradiographs were prepared by technique previously described (see Figures 16, 17, and 18). A uniform distribution of tritium is observed in cleavage region for all of the titanium alloys. The tritium



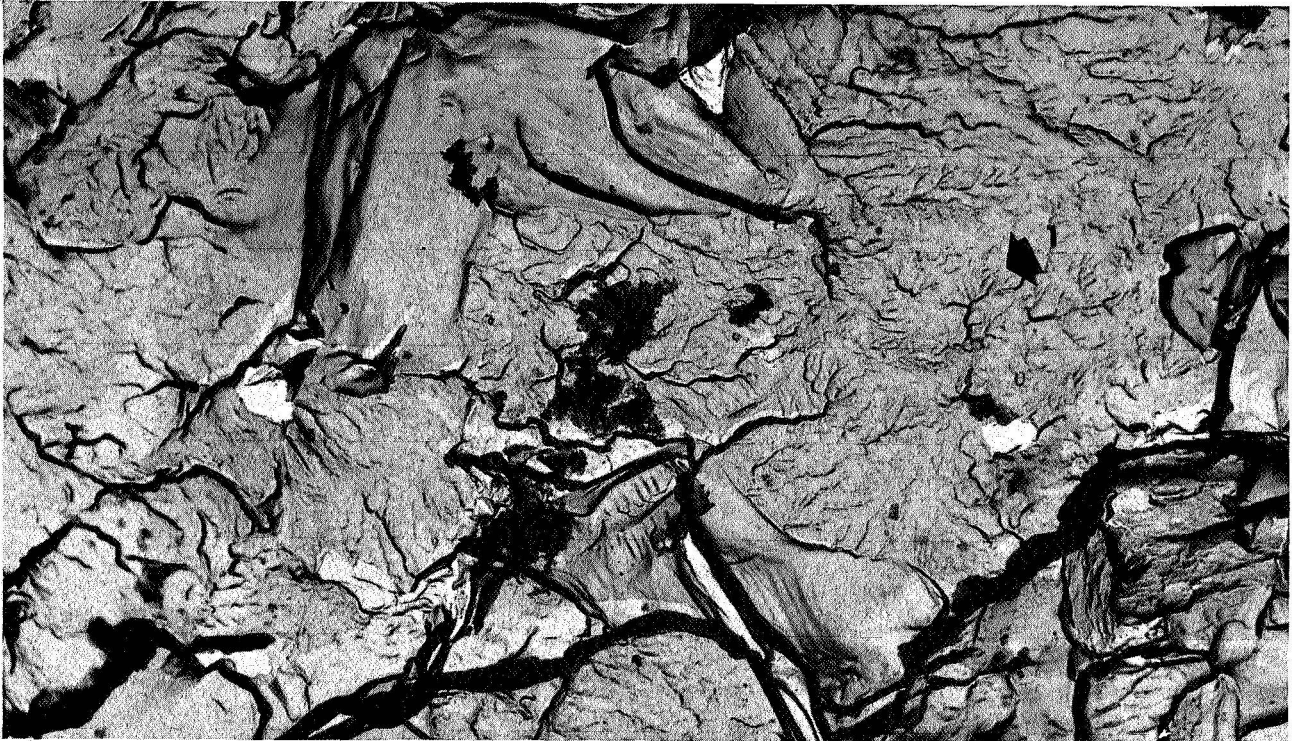
c3870

Figure 12. Electron Microautoradiograph Illustrating Tritium Segregation in Fractured Beta Grain Surface of Ti-6Al-4V Alloy, 30 ppm Tritium Gas Charged and Fractured in Air. Note tritium containing beta phase (1), cleavage regions with river patterns (2), and ductile glide region (3). Magnification 6,000X



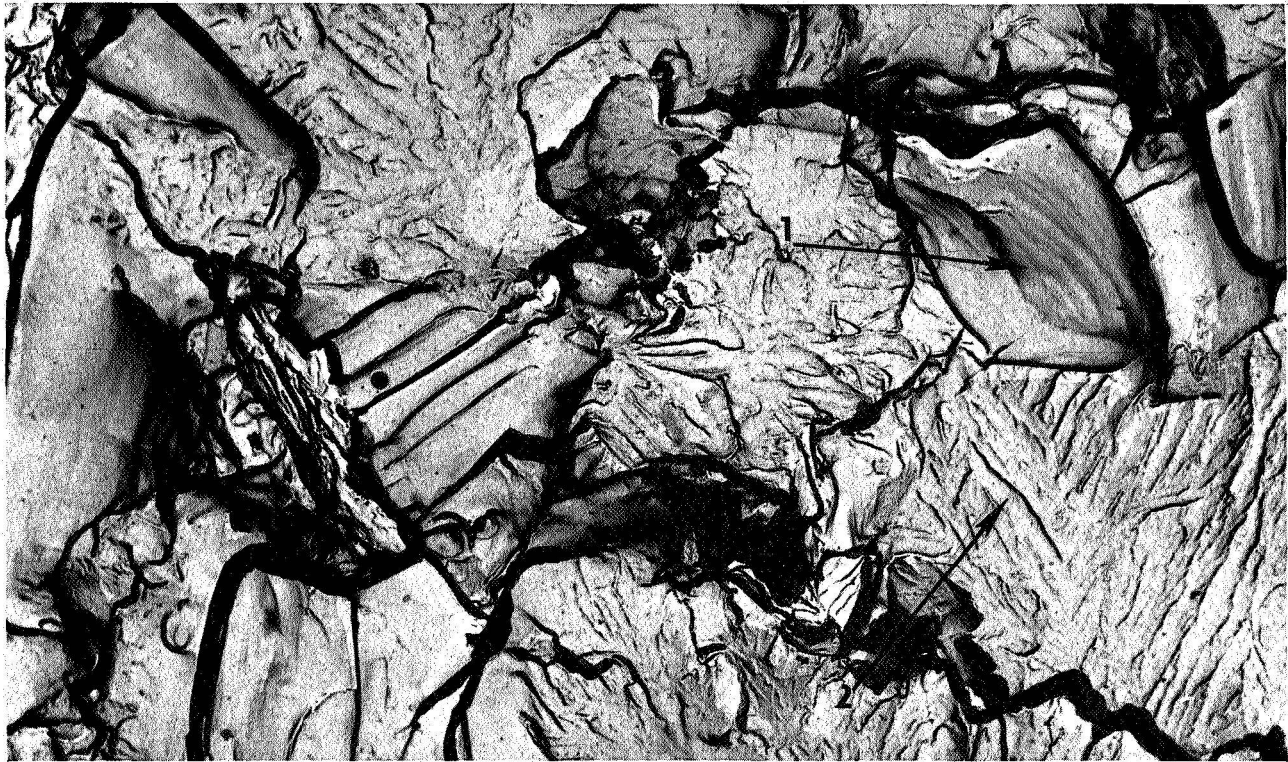
01/22

Figure 13. Electron Microautoradiograph of Ti-8Al-1Mo-1V Alloy, Duplex Annealed, Fracture Face Stress Corrosion Cracked in 2% Tritiated Water. Note ductile glide region, arrow 1, and cleavage region, arrow 2, and absence of tritium. Magnification 12,000X



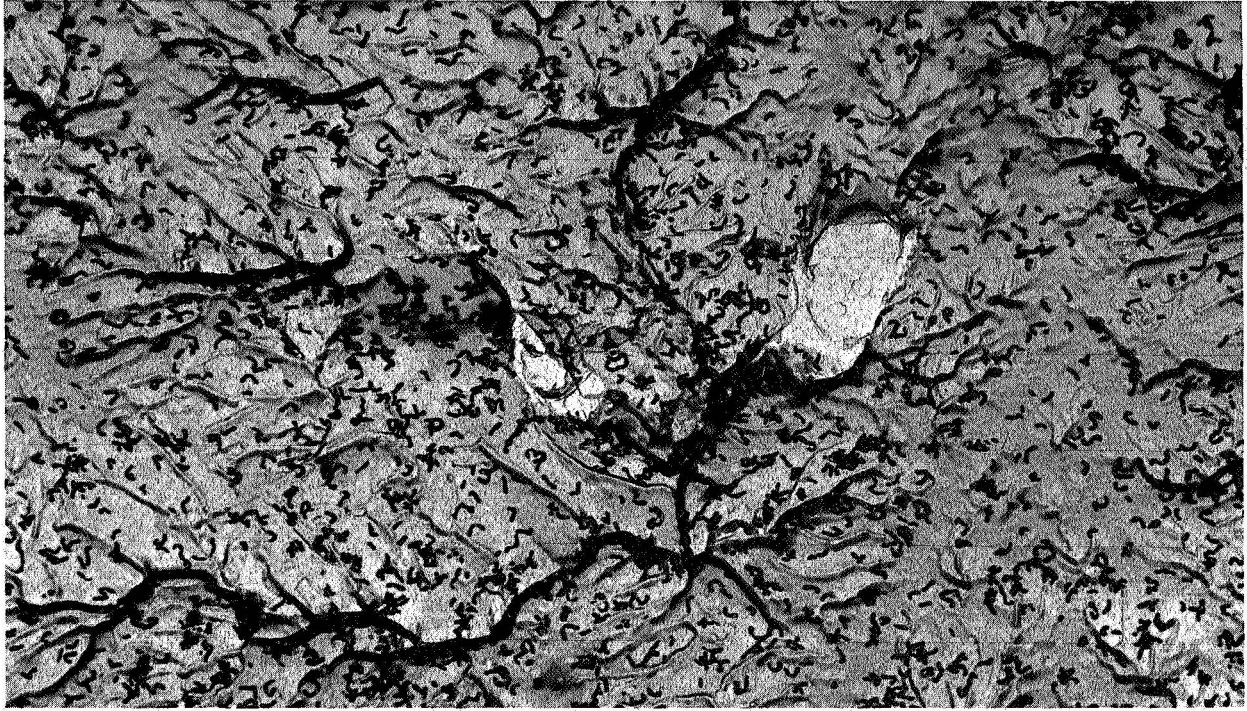
C 4723

Figure 14. Electron Microautoradiograph of Ti-8Al-1Mo-1V Alloy, Duplex Annealed, Fracture Face Stress Corrosion Cracked in 3% Aqueous Salt Solution with 2% Tritiated Water. Note cleavage region, arrow 1 and absence of tritium. Magnification 1200X



c3809

Figure 15. Electron Microautoradiograph of Ti-8Al-1Mo-1V Alloy, 1600°F Solution Annealed, Fracture Face Stress Corrosion Cracked in 3% Aqueous Salt Solution with 2% Tritiated Water. Note ductile glide region, Arrow 1, and cleavage region, Arrow 2, and absence of tritium. Magnification 12,000X



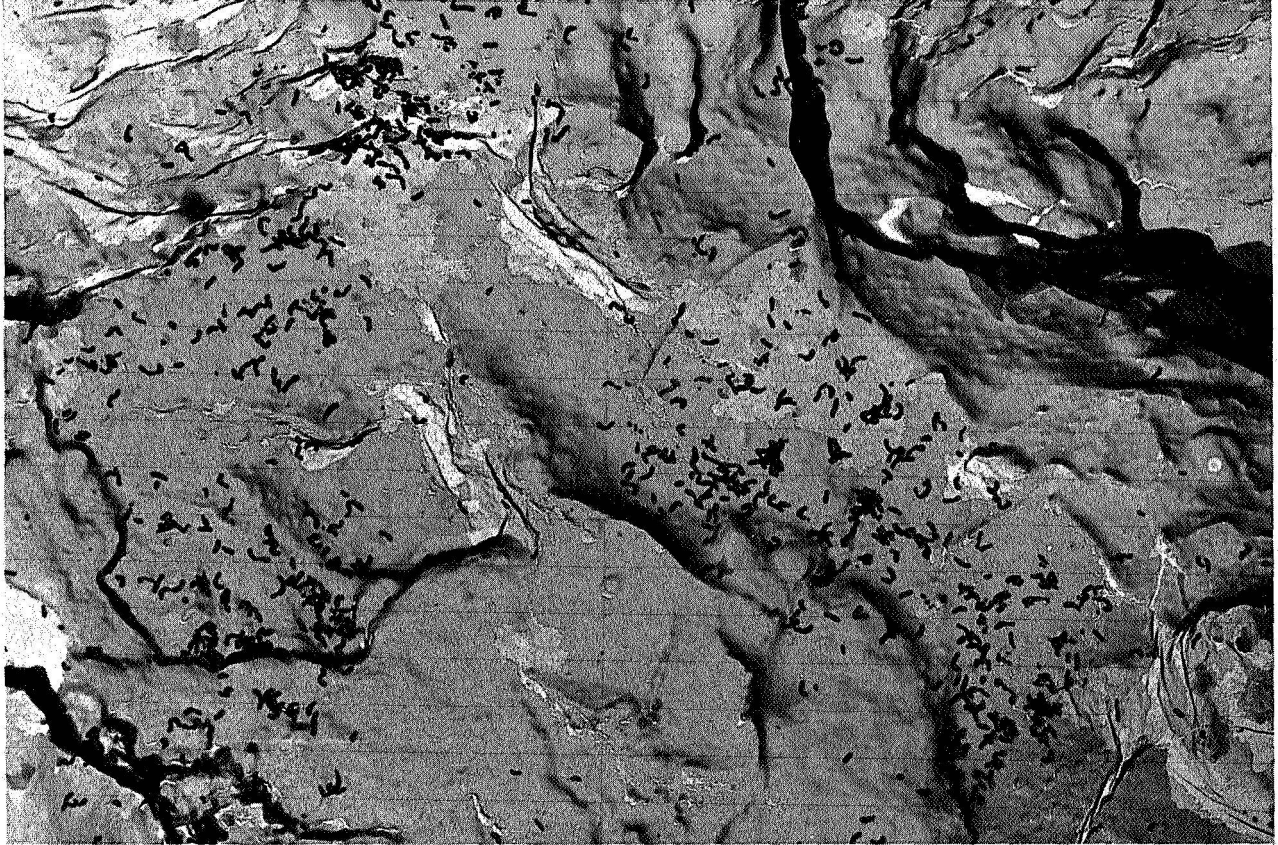
04992

Figure 16. Electron Microautoradiograph of 5 Al-2.5
Charged with 40 ppm Tritium at 1450°F,
Fracture Face Stress Corrosion Cracked in
3% Aqueous Salt Solution. 18000X



c4493

Figure 17. Electron Microautoradiograph of Ti-8Al, Charged with 30 ppm of Tritium at 1450°F, Fracture Face Stress Corrosion Cracked in 3% Aqueous Salt Solution. 12000X



C1111

Figure 18. Electron Microautoradiograph of Ti-8Al-1Mo-1V, Charged with 30 ppm Tritium at 1450°F, Fracture Face Stress Corrosion Cracked in 3% Aqueous Salt Solution. 18000X

concentration in the cleaved region of fractured surfaces is approximately the same as previously reported⁽³⁾ for tritium charged titanium alloys.

2.3 Effect of Aluminum Content on Stress Corrosion Cracking

Alpha titanium alloys Ti-4Al and Ti-8Al and a near alpha alloy Ti-8Al-1Mo sheet were obtained from a program at Battelle Memorial Institute. The alloys were given a six-hour vacuum anneal at 1450^oF to remove hydrogen. For Ti-4Al and Ti-8Al the hydrogen and oxygen impurity levels were determined as 26 ppm H₂, 0.74 w/o O₂, and 8 ppm H₂, 0.76 w/o O₂ respectively. The microstructure of these alpha alloys is shown in Figure 19. The mechanical properties of the Ti-4Al and Ti-8Al are shown in Table V.

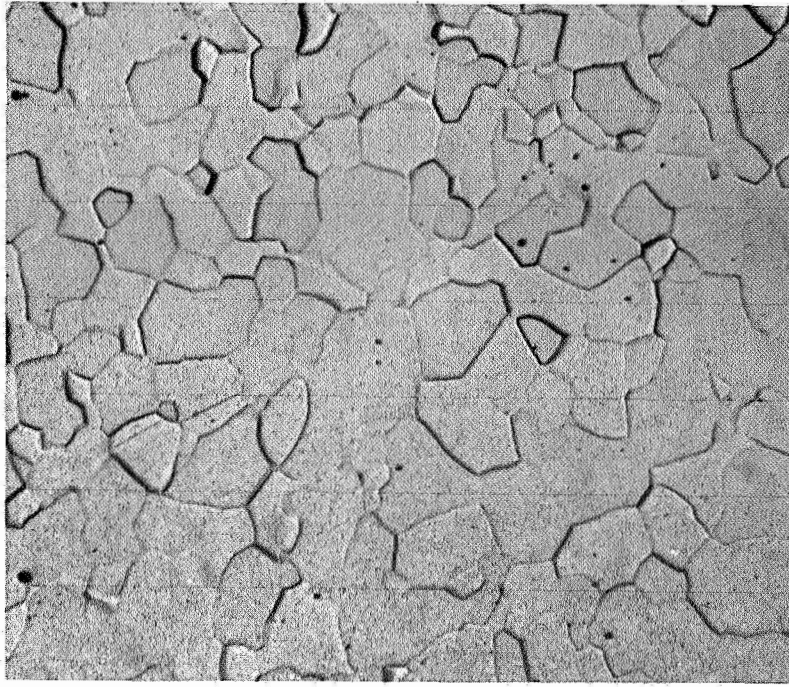
Single-edge notch fracture toughness specimens 0.11" thickness were prepared and tested in 3% NaCl solution. A concentration of 90 and 150 ppm of hydrogen were charged in two specimens of Ti-4Al at 1450^oF. The amount of hydrogen introduced is below the solid solubility for this alloy.⁽⁹⁾ The results are shown in Table VI.

Stress corrosion cracking was not observed in Ti-4Al 3% NaCl solution at ambient temperature. Charging the alloy with hydrogen in the solid solubility range did not introduce SCC. Ti-8Al was quite susceptible to SCC. Water quenching this alloy and Ti-8Al-1Mo from the 1450^oF solution anneal did not improve the stress corrosion behavior. The aluminum content does play an important role in SCC in titanium alloys; however, the ordering reaction in titanium aluminum alloys does not appear to be a requisite for SCC.

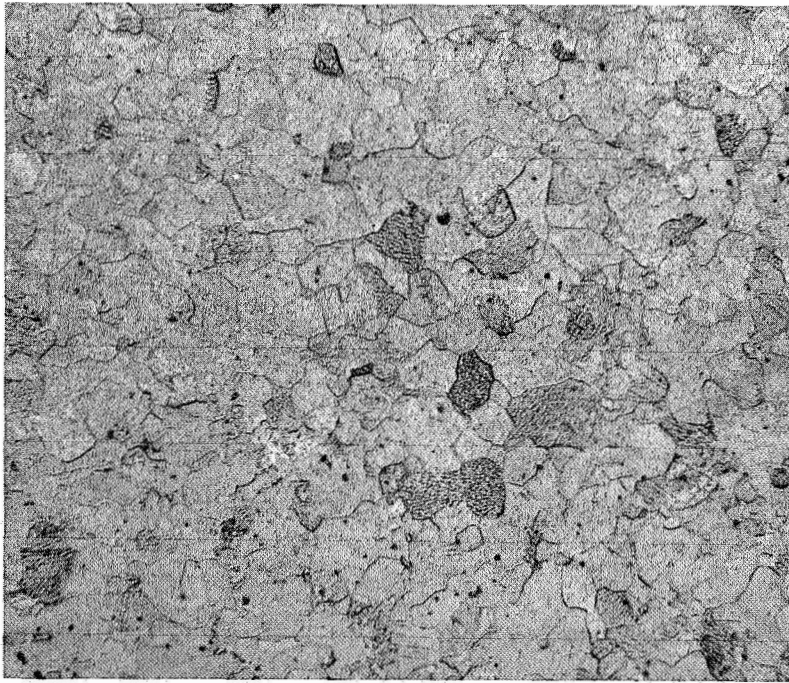
2.4 Transmission Electron Microscopy Studies

Transmission electron microscopy studies were initiated in order to attempt to identify local anodic sites in Ti-5Al-2.5Sn, Ti-8Al-1Mo-1V, and Ti-6Al-4V alloys which showed SCC in salt solutions at ambient temperature.

These experiments required preparation of thin foils of titanium alloys suitable for transmission electron microscopy, examination of foils, dipping the foils in corrosion solution (5% NaCl) for various lengths of time and their re-examination in the electron microscope.



(a)



(b)

(a) Ti-4Al

(b) Ti-8Al

Figure 19. Microstructure of Titanium-Aluminum Alloys
Magnification 200X

TABLE V
MECHANICAL PROPERTIES OF TITANIUM-ALUMINUM
ALPHA ALLOYS

<u>Alloy</u>	<u>Heat Treatment</u>	<u>0.2% Yield ksi</u>	<u>Ultimate Tensile ksi</u>	<u>E1 %</u>	<u>RA %</u>
Ti-4Al	1450 ^o F, 6 hrs, AQ	88	105	24	45
Ti-8Al	1450 ^o F, 6 hrs, AQ	120	133	19	37

TABLE VI
EFFECT OF ALUMINUM CONTENT ON STRESS CORROSION
OF ALPHA TITANIUM

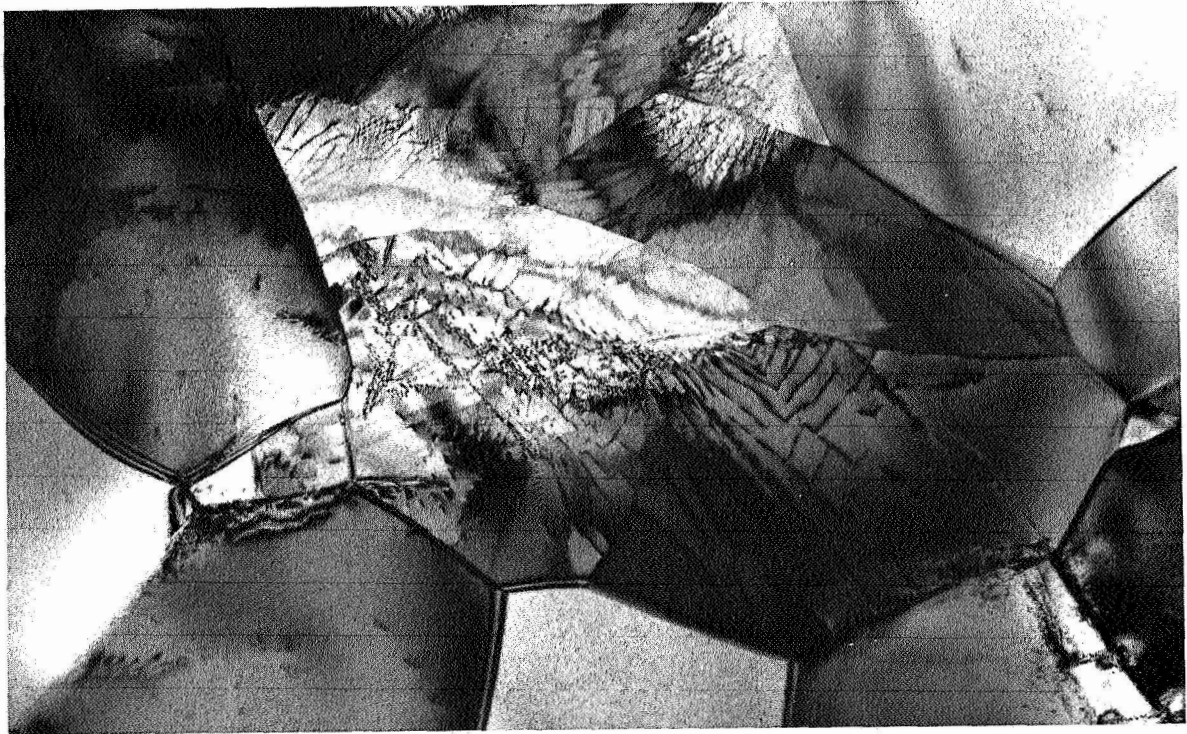
<u>Alloy</u>	<u>Heat Treatment</u>	<u>Environment</u>	<u>Hydrogen Content (ppm)</u>	<u>K_{Ii} ksi √in.</u>	<u>Time to Fracture</u>
Ti-4Al	1450°F, 6 hrs, AQ (vacuum 10 ⁻⁶ torr)	Air	26	62.0	---
	"	3% NaCl	26	62.5	---
	"	"	26	65.3	---
	1450°F, 1 hr, AQ	"	90	61.5	---
	1450°F, 1 hr, AQ	"	150	62.0	---
Ti-8Al	1450°F, 6 hrs, AQ (vacuum 10 ⁻⁶ torr)	Air	8	69.0	---
	"	3% NaCl	8	35.3	2 min.
	1450°F, 6 hrs, WQ	"	8	39.8	3 min.
Ti-8Al-1Mo	1450°F, 6 hrs, AQ	"	---	38.0	20 sec.
	1450°F, 6 hrs, SQ	"	---	20.0	2 min.

Thinning of the titanium alloys was conducted in three steps:

1. Titanium sheet stock was machined to a thickness of .010".
2. Titanium sheets were thinned further in a solution of concentrated HNO₃ and 30% HF which was cooled by an ice bath.
3. Final thinning was done electrolytically in a solution of:
 - 30 ml perchloric acid
 - 295 ml methyl alcohol
 - 75 ml N butyl alcohol

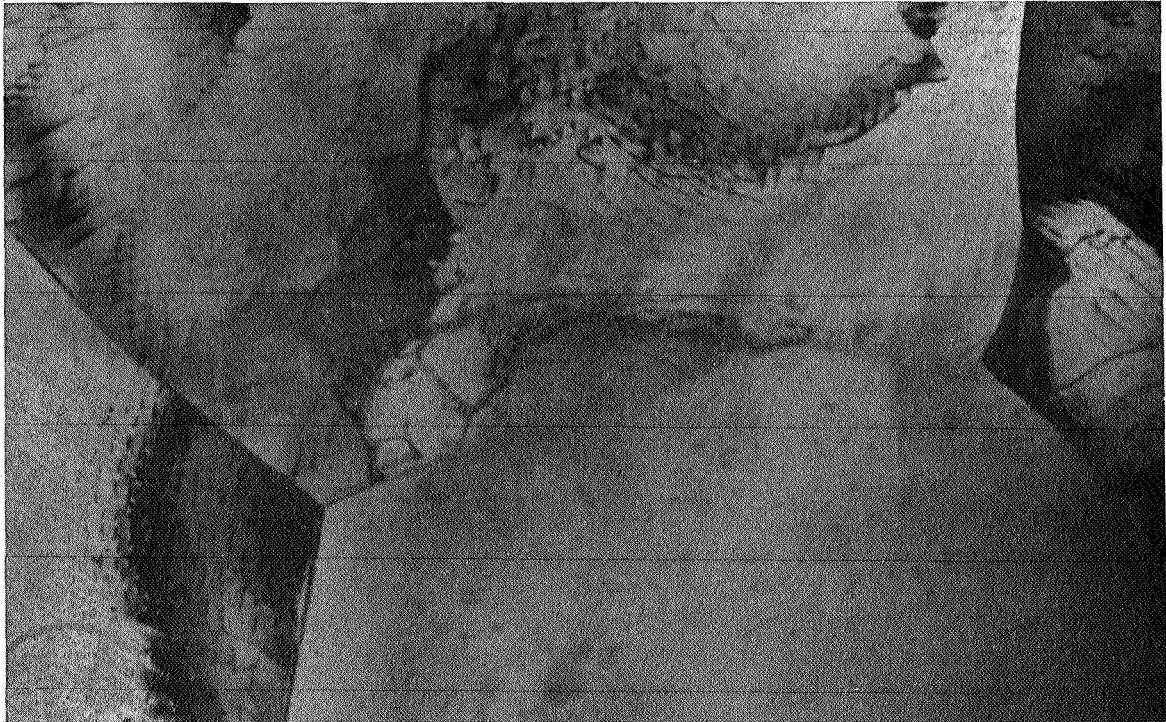
The solution was cooled in a bath of dry ice and acetone and was continuously agitated with a magnetic stirrer. Thinning occurred most rapidly on foil at air-solution interface; therefore the foils were moved up and down using an electric motor-crank device at 30 immersions per minute. This was done for the first ten minutes of electrolytic thinning. The final ten minutes was conducted without dipping to remove any possible atmospheric contamination. This technique produced foils without contamination and afforded large areas thin enough for transmission. Figures 20, 21, and 22 show transmission electron micrographs of Ti-8Al-1Mo-1V, Ti-6Al-4V, and Ti-5Al-2.5Sn. The dislocation structure was similar for all of the titanium alloys. Some of the grains were free of dislocations while the surrounding grains contained dislocation networks.

Thin foils of Ti-8Al-1Mo-1V, Ti-6Al-4V, and Ti-5Al-2.5Sn were immersed and stressed in 5% NaCl for various lengths of times. The foil was placed between two titanium grids, immersed in 5% salt solution, and stressed by bending the titanium grids to a U shape. After immersion, the foils were re-examined in the electron microscope. Figure 23 shows the exact electron micrograph as shown in Figure 22 after two minutes immersion in 5% salt solution. Figures 24 and 25 show transmission electron micrographs of Ti-8Al-1Mo-1V and Ti-6Al-4V following 8-minute and 45-minute immersion in 5% salt solution. From these experiments no evidence was found for any pitting action on foils by 5% NaCl solution. Possibly, insufficient strain was present to rupture the oxide film and expose fresh metal surface to corrosion environment.



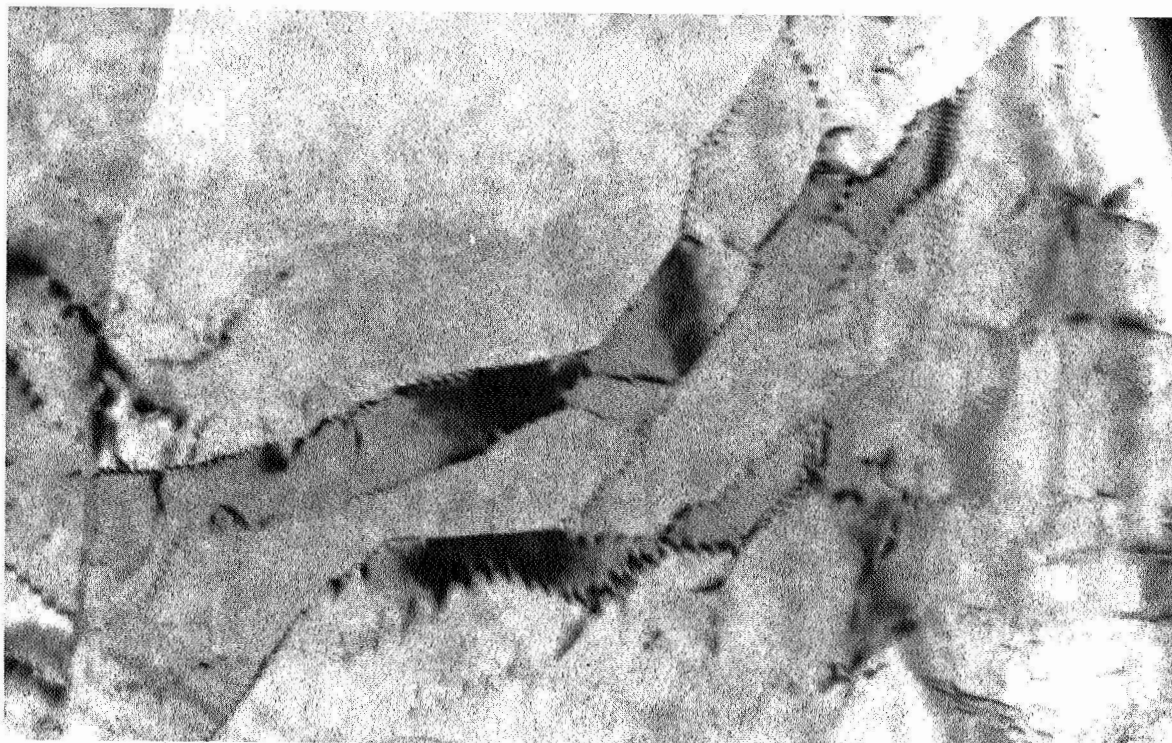
c3619

Figure 20. Transmission Electron Micrograph of Ti-8Al-1Mo-1V, Duplex Annealed. 28,000X



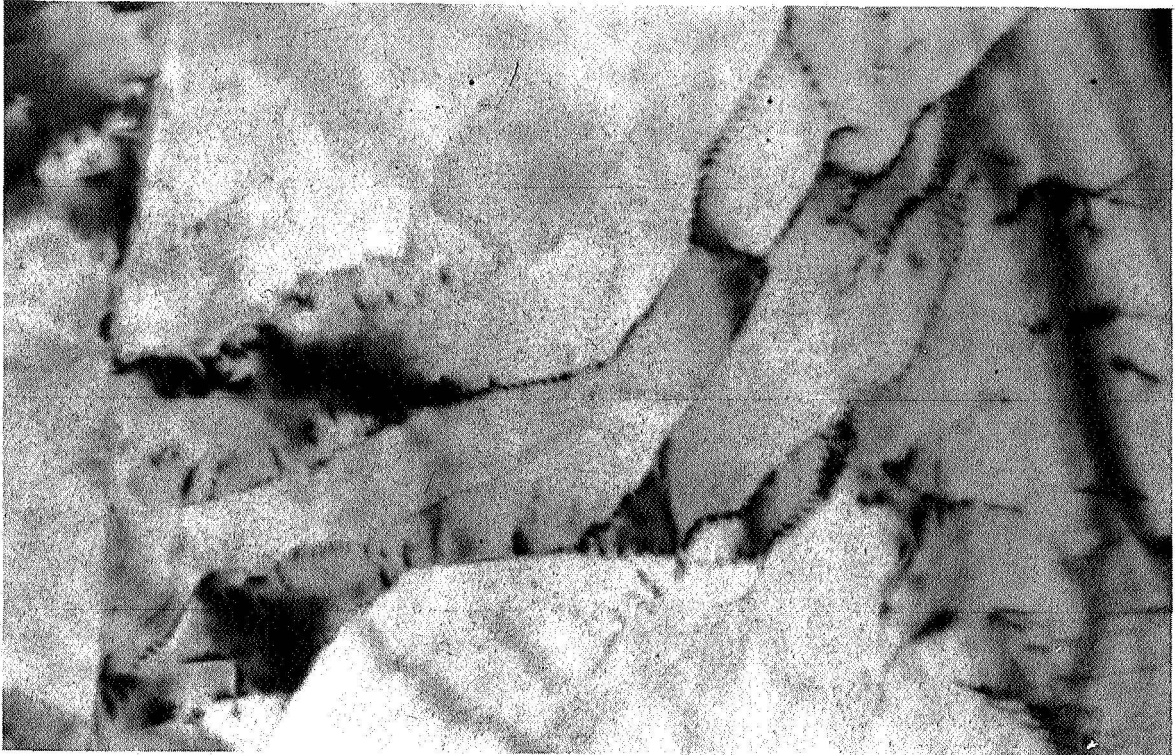
c3620

Figure 21. Transmission Electron Micrograph of Ti-6Al-4V. 28,000X



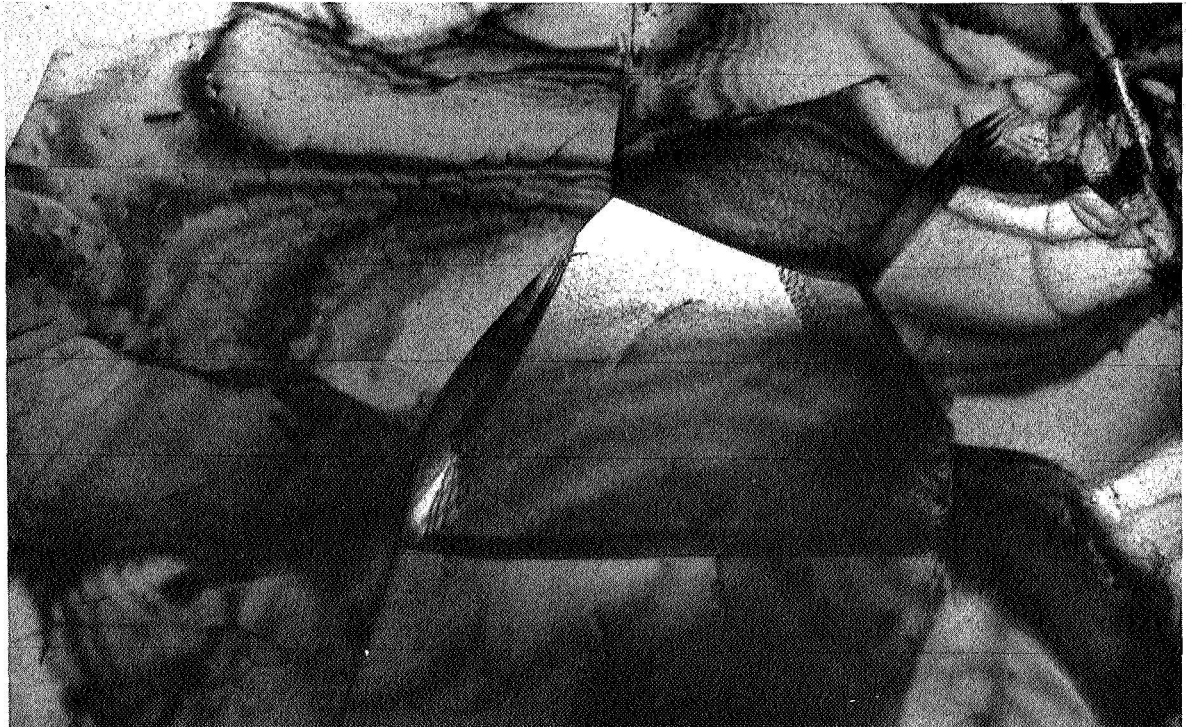
c362/

Figure 22. Transmission Electron Micrograph of
Ti-5Al-2.5Sn. 28,000X



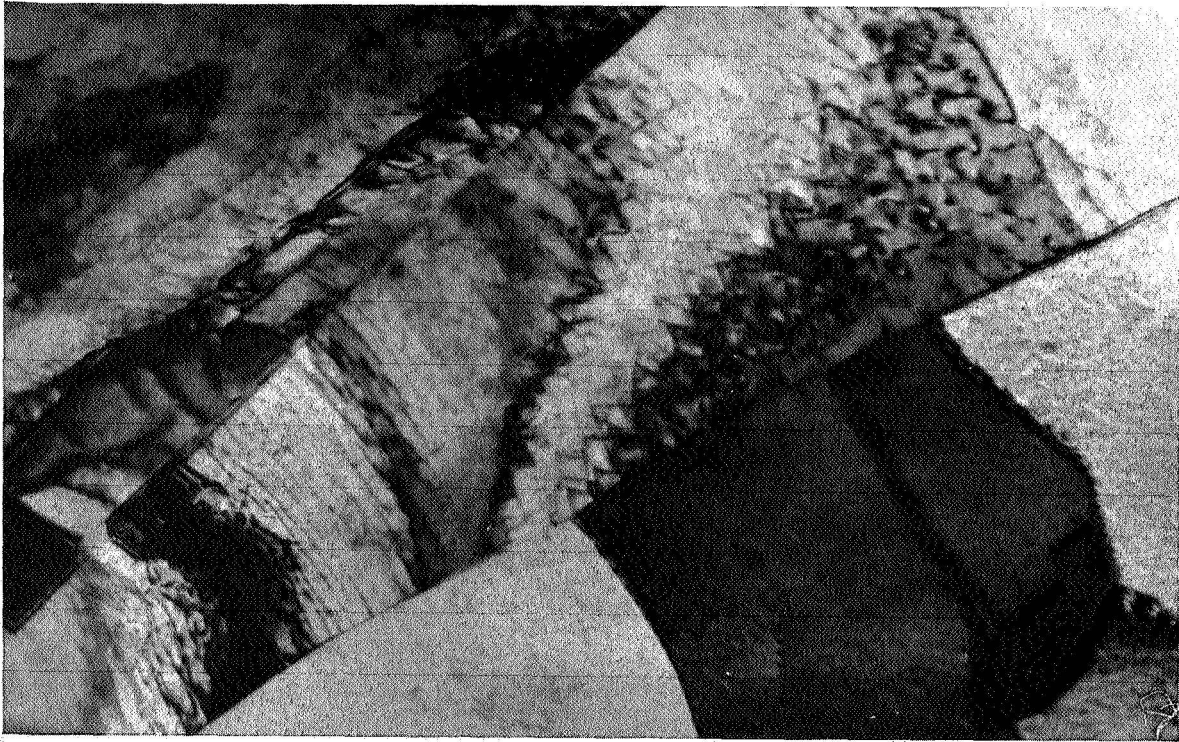
C3622

Figure 23. Transmission Electron Micrograph of Ti-5Al-2.5Sn Following Stress and 2-Minute Immersion in 5% NaCl Solution. 28,000X



43623

Figure 24. Transmission Electron Micrograph of Ti-8Al-1Mo-1V Following Stress and 8-Minute Immersion in 5% NaCl Solution. 28,000X



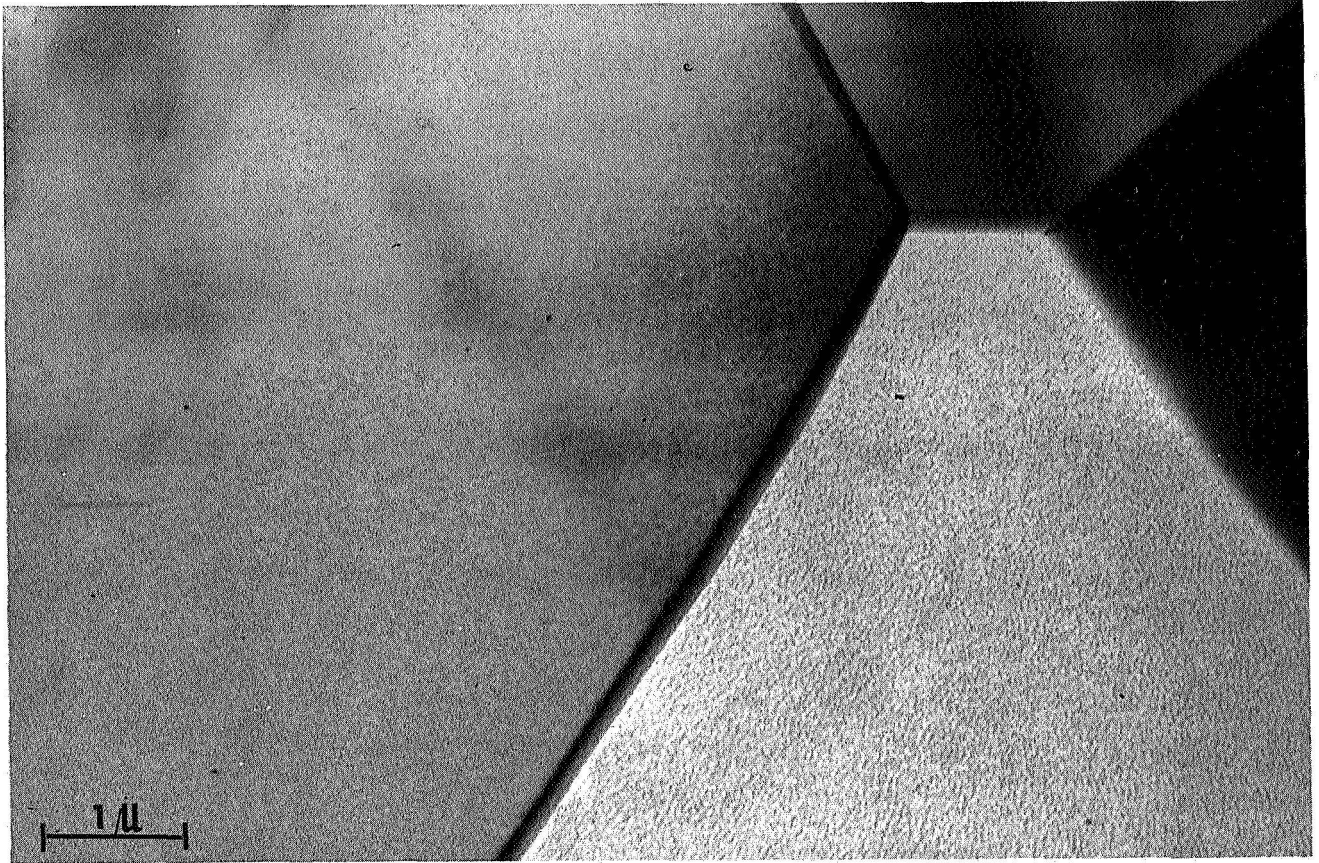
63624

Figure 25. Transmission Electron Micrograph of Stressed Ti-6Al-4V Following Stress and 45-Minute Immersion in 5% NaCl Solution. 28,000X

Swann⁽¹⁰⁾ emphasized that alloys with a cellular arrangement of dislocation tangles have superior resistance to transgranular failure, whereas alloys containing planar groups of dislocations are generally more susceptible. Blackburn⁽¹¹⁾ has shown that dislocation arrangements vary from cellular arrays in unalloyed, low oxygen titanium to coplanar arrays in 9 w/o Al alloy. The transition from cellular to coplanar arrays occurs at an aluminum content of 5 w/o Al.

Transmission studies of Ti-4Al, Ti-8Al, and Ti-8Al-1Mo-1V were made in annealed and deformed condition. Ti-8Al specimens were water quenched from 1450°F to obtain disordered state. Ti-8Al-1Mo-1V was studied in duplex annealed, 1800°F and 2000°F annealed condition.

Figures 26 and 27 show transmission electron micrograph of annealed Ti-4Al and Ti-8Al respectively. The dislocation free alpha alloy is typical for both Ti-4Al and Ti-8Al. Figures 28 and 29 show dislocation tangles for Ti-4Al which had been deformed approximately 10%. Figure 30 shows dislocation arrangement in Ti-8Al following 10% deformation. The planar groups of dislocation are typical for this alloy in disordered state. The dislocation arrangement for Ti-8Al-1Mo-1V duplex annealed with approximately 15% strain is shown in Figures 31 and 32. The planar dislocation arrangement in alpha phase of Ti-8Al-1Mo-1V duplex annealed was similar to Ti-8Al alloy. Figure 33 shows transmission electron micrograph of dislocation free Ti-8Al-1Mo-1V beta annealed from 2000°F. The dislocation arrangement for this alloy when deformed approximately 5% is shown in Figure 34. The planar dislocation arrangement in acicular martensitic alpha phase is pinned by the retained beta phase. Figure 35 shows transmission electron micrograph at approximately 8% deformation; slip is observed across several grains of retained beta and martensitic alpha phase. This type of slip is also observed in script type islands of Ti-8Al-1Mo-1V quenched from 1800°F (see Figure 36).



64495

Figure 26. Transmission Electron Micrograph of Annealed Ti-4Al Alloy. Note Dislocation Free Structure.

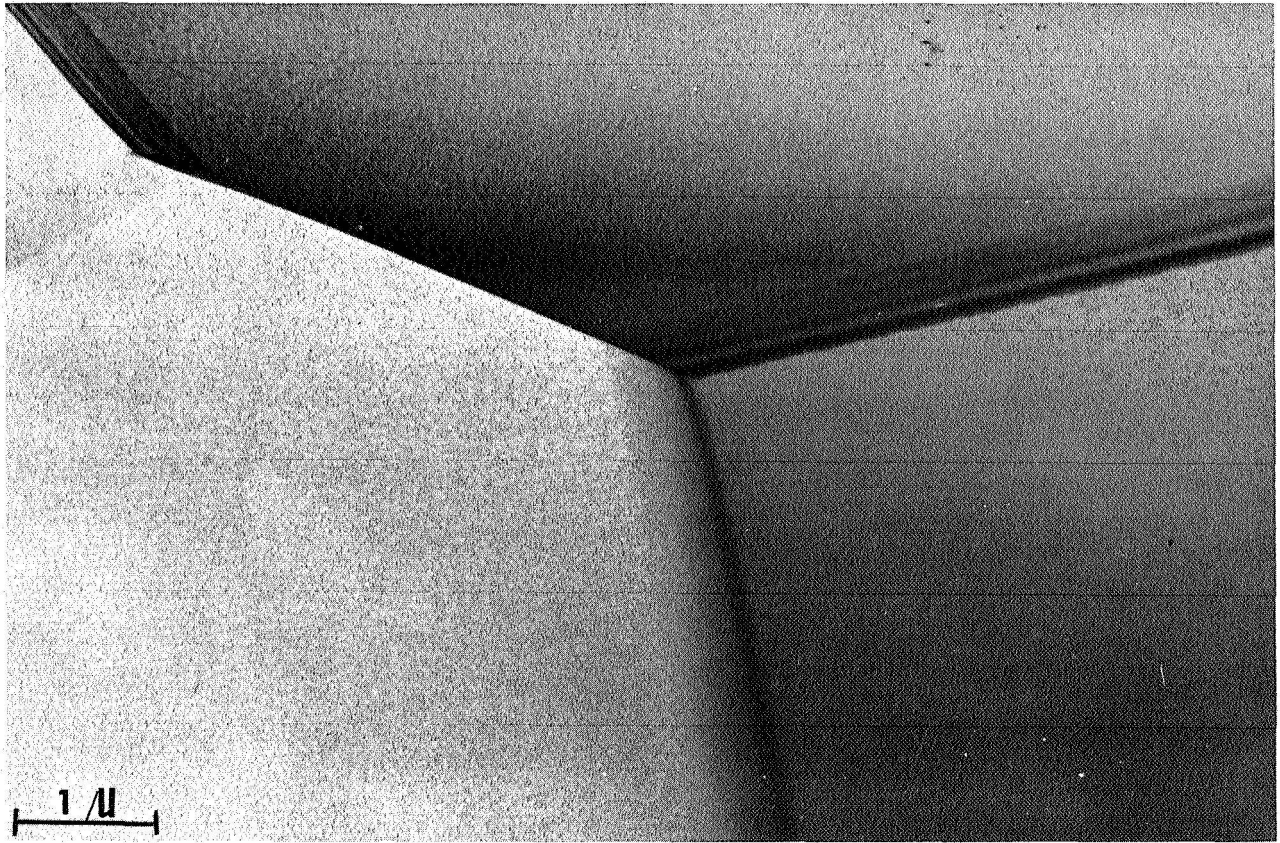
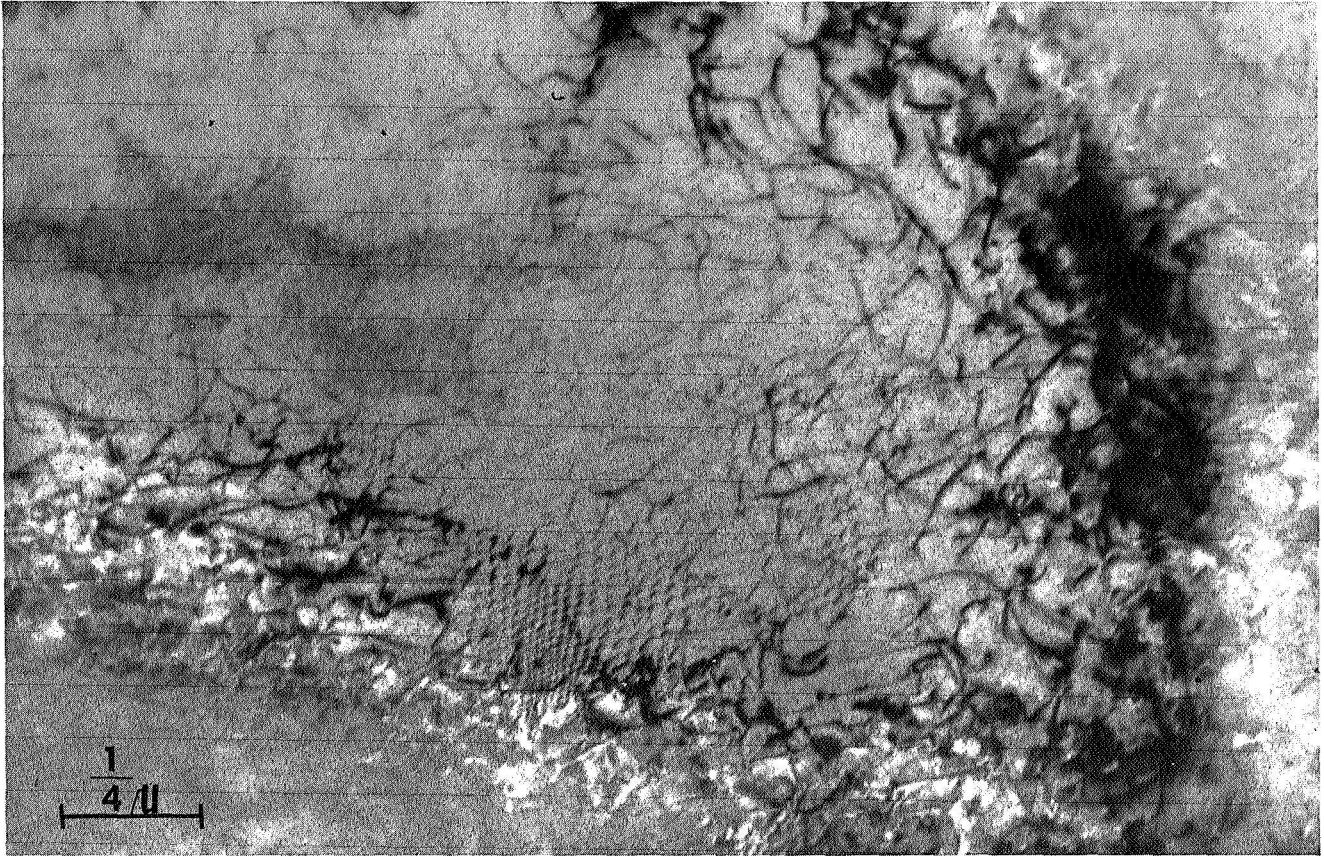


Figure 27. Transmission Electron Micrograph of Annealed Ti-8Al Alloy. Note Dislocation Free Structure.



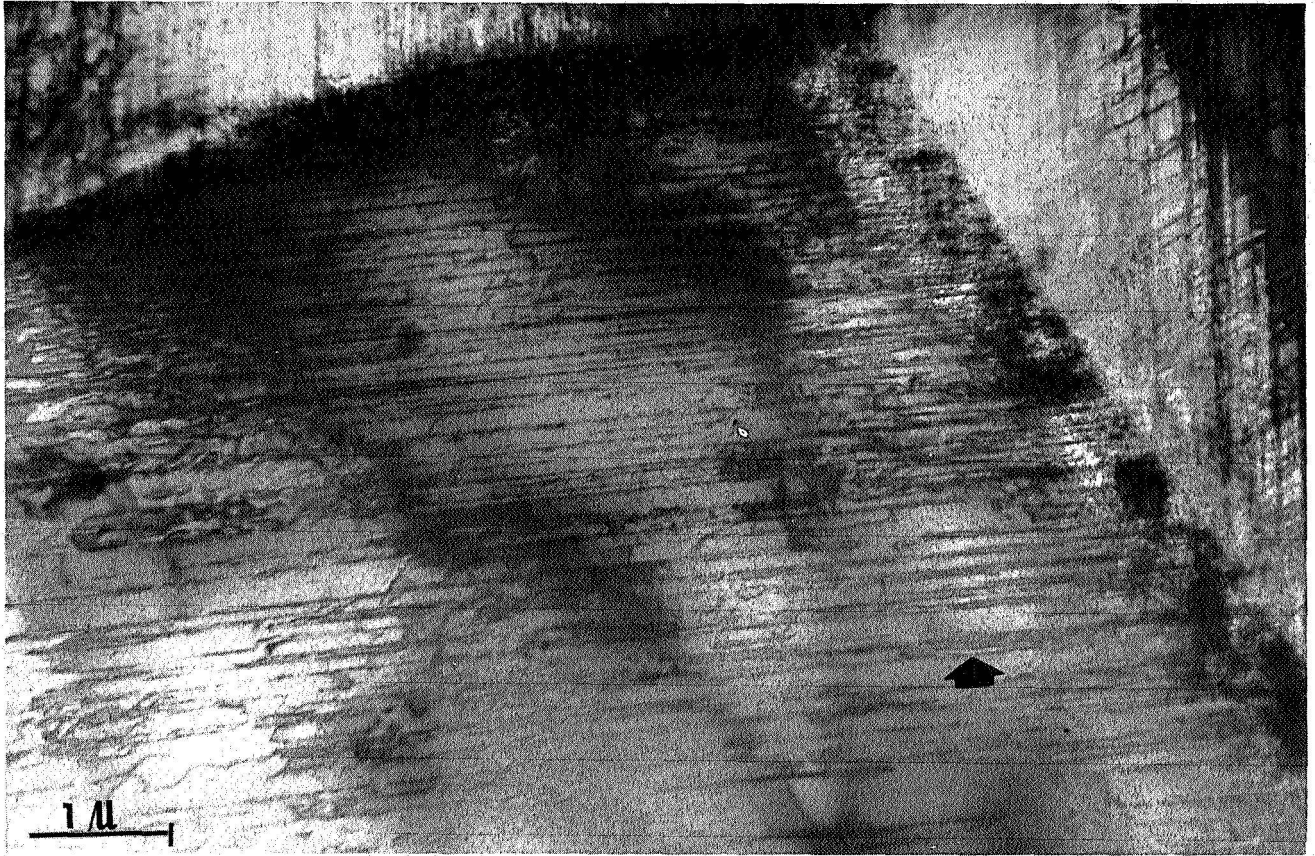
c4497

Figure 28. Transmission Electron Micrograph of Ti-4Al Strained Approximately 10%. Note Dislocation Tangles - Arrows.



c4498

Figure 29. Transmission Electron Micrograph of Ti-4A Strained Approximately 10%. Note Dislocation Tangles.



04499

Figure 30. Transmission Electron Micrograph of Ti-8Al Deformed Approximately 10%. Note Slip Planes - Arrow.

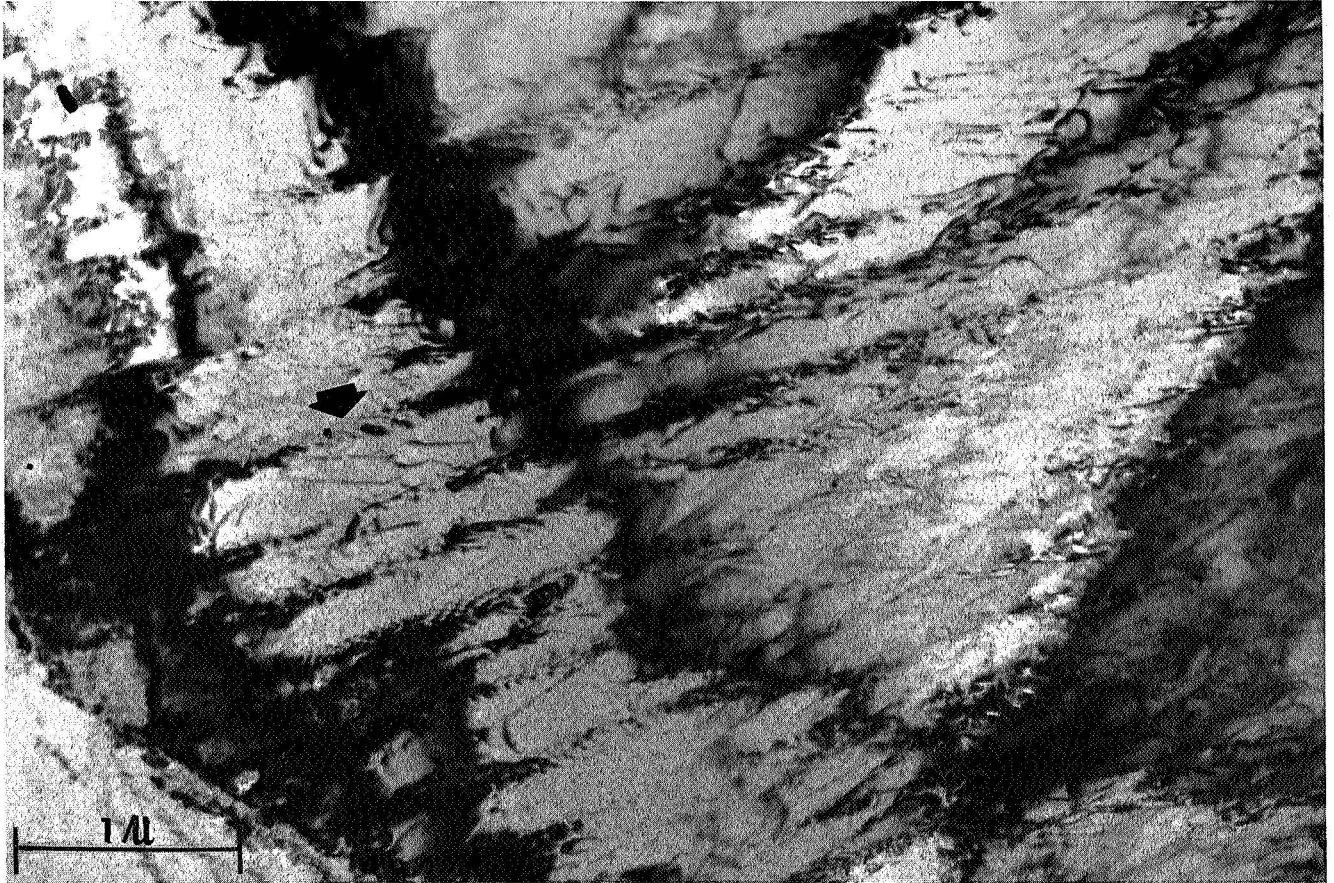
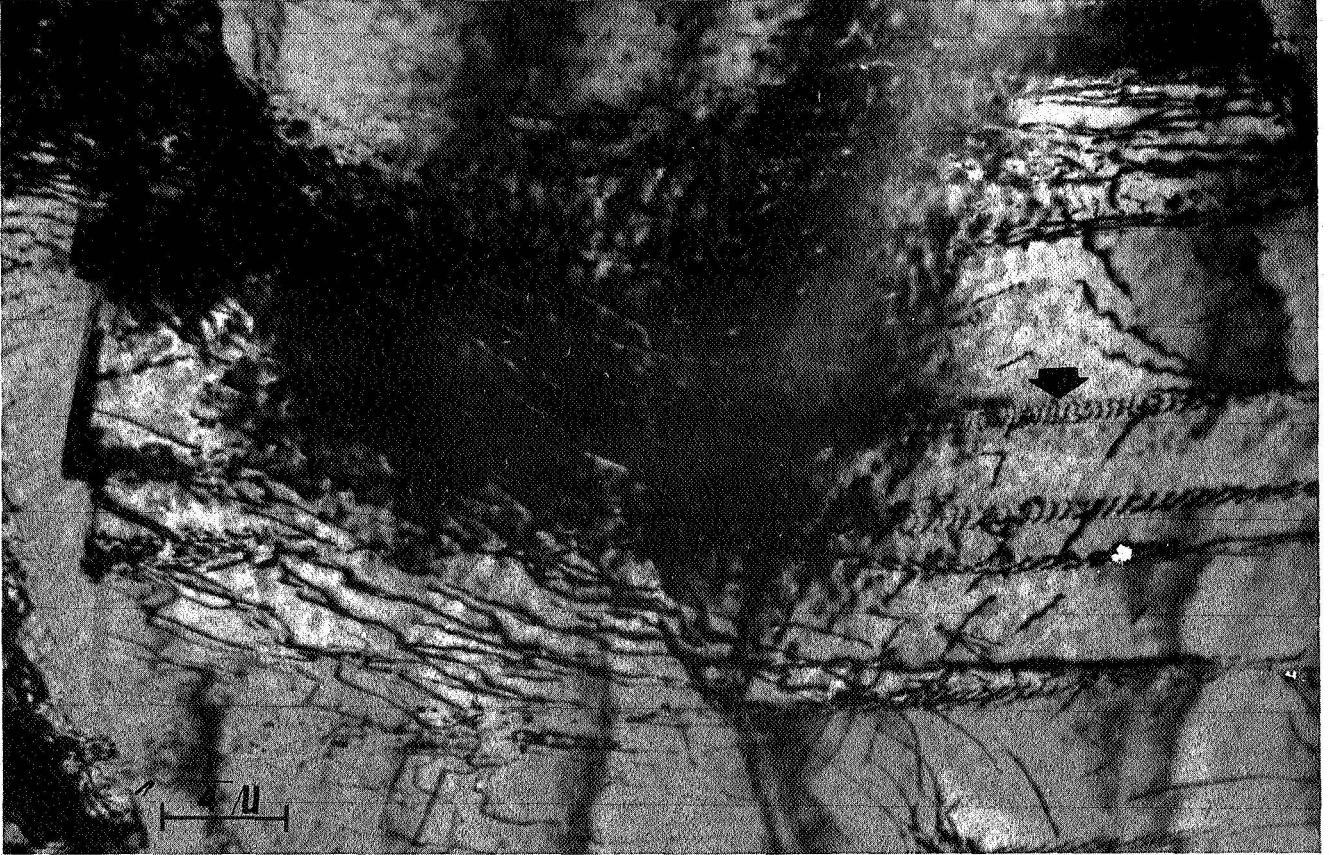
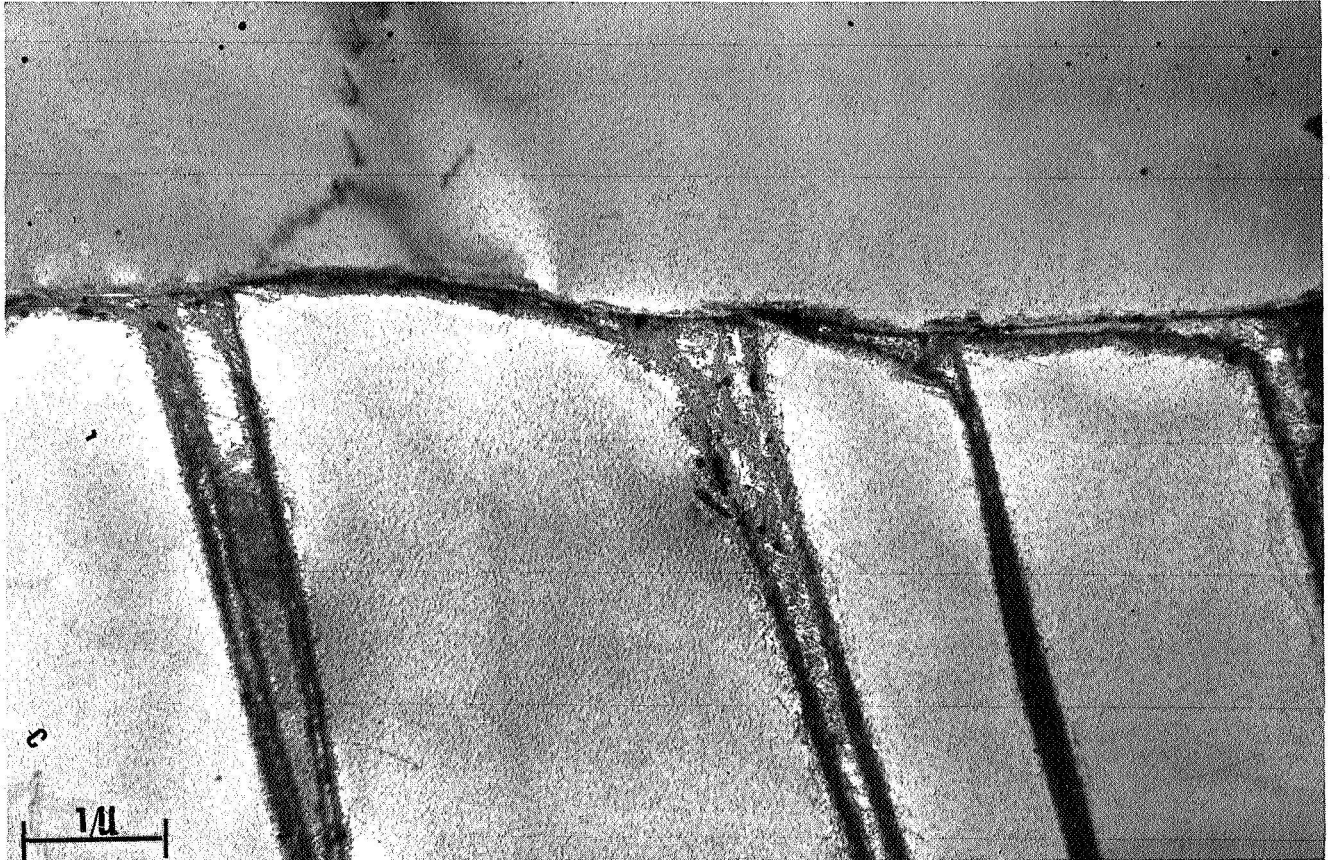


Figure 31. Transmission Electron Micrograph of Ti-8Al-1Mo-1V Duplex Annealed, Strained Approximately 15%. Note Slip Planes - Arrow.



ey501

Figure 32. Transmission Electron Micrograph of Ti-8Al-1Mo-1V Duplex Annealed Strained Approximately 15%. Note Coplanar Array of Dislocations - Arrow.



44502

Figure 33. Transmission Electron Micrograph of Ti-8Al-1Mo-1V Solution Annealed at 2000°F, Air Quenched. Note Dislocation Free Material.



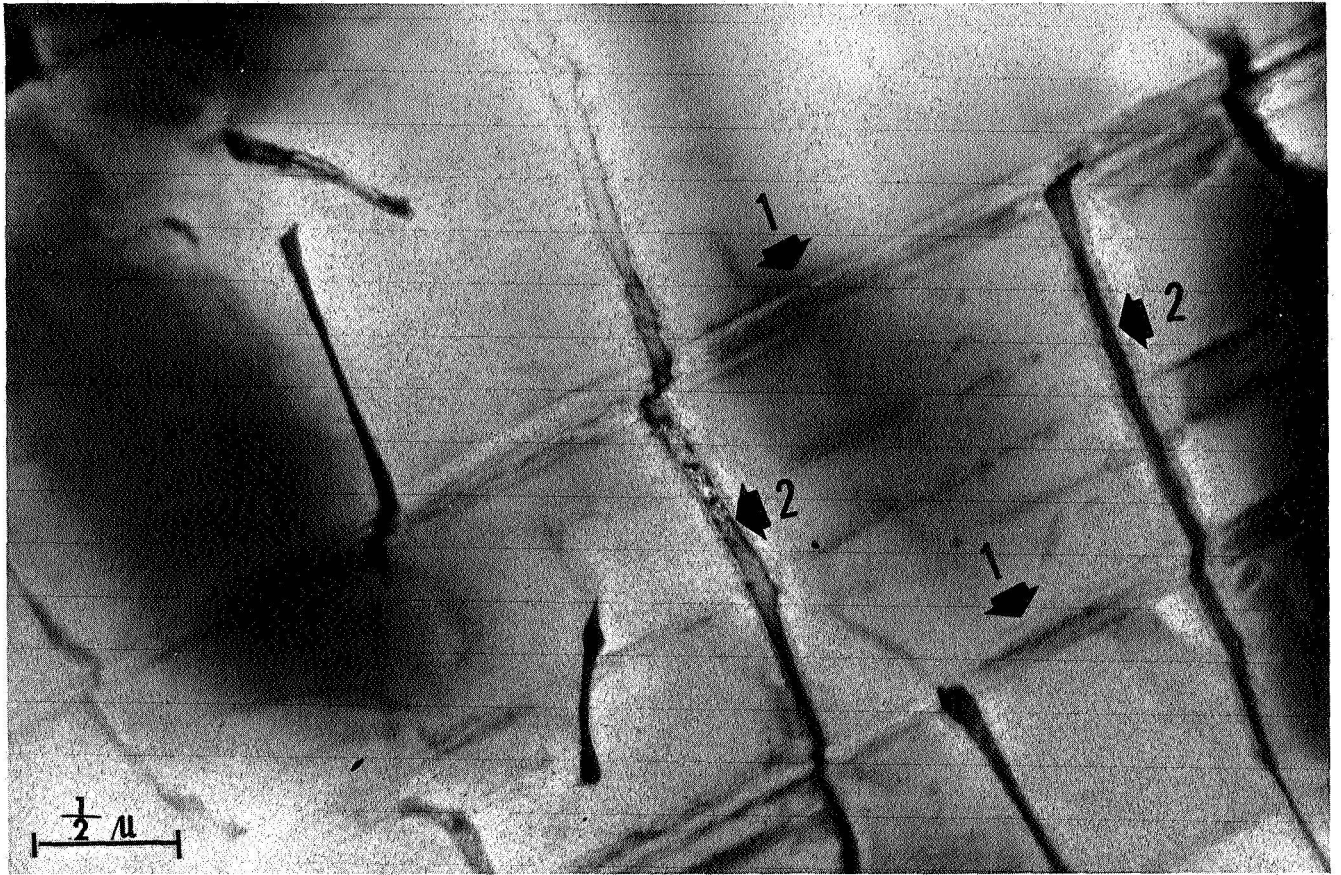
C4503

Figure 34. Transmission Electron Micrograph of Ti-8Al-1Mo-1V Solution Annealed at 2000°F, Air Quenched, Strained Approximately 5%. Note Retained Beta, Arrow 1, Coplanar Dislocation Arrangement, Arrow 2.



c4504

Figure 35. Transmission Electron Micrograph of Ti-8Al-1Mo-1V Solution Annealed at 2000°F, Air Quenched, Strained Approximately 8%. Note Slip Planes in Martensitic Alpha, Arrow 1, Deformation in Retained Beta, Arrow 2.



04506

Figure 36. Transmission Electron Micrograph of Ti-8Al-1Mo-1V Solution Annealed at 2000°F, Air Quenched, Deformed Approximately 8%. Note Slip Planes, Arrow 1, Retained Beta, Arrow 2.

3.0 CONCLUSIONS

The results obtained from the current investigation, and the conclusions reached are summarized below.

1. Precracked notched alpha beta type Ti-8Al-1Mo-1V in duplex annealed, 1600°F, and 1700°F solution annealed were susceptible to stress corrosion cracking in aqueous salt solution at ambient temperature.
2. Martensitic structures obtained by annealing specimens at 1800°F or higher, and containing hydrogen up to 100 ppm, were immune to SCC in aqueous salt solutions.
3. The susceptibility to SCC of alpha beta structures, obtained by reheating martensitic structures from 1800°F in the temperature range 900°F to 1450°F, was dependent on the strain rate.
4. The specimens of Ti-8Al-1Mo-1V alloy stress corrosion cracked in distilled water with 2% tritiated water and in 3% NaCl solution with 2% tritiated water did not appear to exhibit evidence of hydrogen (tritium) diffusion into the substrate metal from the fractured face by electron microautoradiography. If the alloy sample retained tritium below the surface layer, it could easily be detected by this method. The diffusion coefficient usually is temperature dependent. Measurements made during degassing studies indicated $0.7 \times 10^{-5} \text{ cm}^2/\text{sec}$ at 1100°F, and $2.6 \times 10^{-5} \text{ cm}^2/\text{sec}$ at 1470°F for pure Ti. (13, 14) Extrapolation of these values to an ambient temperature of 25°C gives $1.8 \times 10^{-11} \text{ cm}^2/\text{sec}$. These are several orders of magnitude lower than diffusion of H in titanium at elevated temperatures and would not be rate controlling for hydrogen permeation into metal. It is difficult to reconcile these data with the hydrogen embrittling theory of SCC. Surface reactions appear to be important in this relation.
5. Aluminum plays an important role in SCC of titanium. The alpha alloy Ti-4Al, containing up to 150 ppm hydrogen was immune to SCC. The alpha alloy Ti-8Al whether air quenched or water quenched from 1450°F was susceptible to SCC.
6. Increasing the aluminum content above 5% changes dislocation arrangement from cellular arrays to coplanar arrays. Coplanar dislocation arrays are commonly associated with SCC. Aluminum appears to lower the stacking fault energy with slip occurring along preferred crystallographic planes. In acicular martensitic structure planar dislocation arrays were also observed in strained Ti-8Al-1Mo-1V, however, the retained beta pins the dislocation movement. Deformation in this heat treated condition occurs by simultaneous slip across several acicular needles. The restricted deformation of the martensitic

alpha phase by retained beta appears to be causing immunity to SCC. The conclusion of Lane and Cavallaro⁽¹²⁾ that the formation of the coherent Ti_3Al precipitate is necessary for SCC does not appear to be a valid conclusion.

REFERENCES

1. "Aircraft Designers Handbook for Titanium and Titanium Alloys," Technical Report AFML-TR-67-142, Defense Metals Information Center, March 1967.
2. J. C. Scully, "Kinetic Features of Stress Corrosion Cracking," a paper presented at Fundamental Aspects of Stress Corrosion Cracking Conference, Ohio State University, September 1967.
3. T. L. Mackay and C. B. Gilpin, "Stress Corrosion Cracking of Titanium Alloys at Ambient Temperature in Aqueous Solutions," Report SM-49105-F1, NAS 7-488, July 1967.
4. T. R. Beck, "Stress Corrosion Cracking of Titanium Alloys, Heat Treatment Effects, Stress Corrosion Cracking in Various Solvents and Electrochemical Kinetics with Ti-8Al-1Mo-1V Alloy," Contract NAS 7-489, Progress Report No. 2, December 1966.
5. R. E. Curtis and W. F. Spurr, Trans. Am. Soc. Metals, 51, (1968), p. 115.
6. J. E. Srawley and W. F. Brown, Jr., "Fracture Toughness Testing Methods," ASTM STP 381, April 1965.
7. B. F. Brown and C. D. Beachem, Corrosion Science, 5, 1965, p. 745.
8. M. J. Blackburn, Trans. Am. Soc. Metals, 59, (1966), p. 876.
9. L. W. Berger, D. N. Williams, and R. I. Taffee, Trans. AIME, 212, (1958), p. 509.
10. P. R. Swann, Corrosion, 19, (1963) p. 102
11. M. J. Blackburn, Trans. Am. Soc. Metals, 59, (1966) p. 694.
12. I. R. Lane and J. L. Cavallaro, "Metallurgical and Mechanical Aspects of the Sea-Water Stress Corrosion of Titanium," Applications Related Phenomena in Titanium Alloys, ASTM STP 432 American Society for Testing and Materials, 1967, p. 147.
13. R. J. Wasilewski and G. L. Kehl, "Diffusion of Hydrogen, Nitrogen and Oxygen in Titanium," Summary Report from Columbia University to Watertown Arsenal Laboratory, Contract No. Da-30-069-ORD-644, July 13, 1953.
14. D. N. Williams, F. R. Schwaberg, P. R. Wilson, W. M. Albrecht, M. W. Mallet and R. I. Jaffee, "Hydrogen Contamination in Titanium and Titanium Alloys, Report from Battelle Memorial Institute to Wright Air Development Center, Contract AF33(616)-2873, March 1957.

